NATURE AND ORIGIN OF MINERAL COATINGS ON VOLCANIC ROCKS OF THE BLACK MOUNTAN, STONEWALL MOUNTAIN, AND KANE SPRINGS WASH VOLCANIC CENTERS, SOUTHERN NEVADA

Dr. James V. Taranik, Principal Investigator
Dr. Liang C. Hsu, Co-Investigator
David Spatz, Co-Investigator

Mackay School of Mines
Department of Geological Sciences
University of Nevada, Reno
Reno, Nevada 89557

January, 1988
Semiannual Progress Report for Period July, 1987 - January, 1988

Contract Number NAS5-28765

(NASA-CR-181437) NATURE AND ORIGIN OF MINERAL COATINGS ON VOLCANIC ROCKS OF THE BLACK MOUNTAIN, STONEWALL MOUNTAIN, AND KANE SPRINGS WASH VOLCANIC CENTERS, SOUTHERN NEVADA Semiannual Progress Report, Jul. 1987 G3/46

N88-17140

Unclas
0123411

Prepared for
The National Aeronautics and Space Administration
Goddard Space Flight Center
Greenbelt, Maryland 20771

TABLE OF CONTENTS

TM SPECTRAL CHARACTERISTICS AND IMAGERY ANALYSIS, VOLCANIC ROCK ASSEMBLAGES, SOUTHERN NEVADA

D.M. Spatz, J.V. Taranik, L.C. Hsu

ABSTRACT

Comparative lab spectra and Thematic Mapper imagery investigations at 3 Tertiary calderas in southern Nevada indicate that desert varnish is absorbant relative to underlying host rocks below about 0.7 to 1.3 micrometers, depending on mafic affinity of the sample, but less absorbant than mafic host rocks at higher wavelengths. In some cases the distinction is lost at higher wavelengths (bands 5 and 7). Desert varnish occurs chiefly as thin impregnating films. Distribution of significant varnish accumulations + over 5 micrometer thicknesses - is sparse and localized, occuring chiefly in surface recesses. These relationships result in dominance of lithologic spectral responses in the longer wavelength bands and high 5/2 values over felsic units with extensive desert varnish coatings.. Highly evolved magmatic differentiates with peralkaline tendencies and a high proportion of incompatible elements which partition into residual melt exhibit characteristic spectra. These units are unusually reflectant in band 7, leading to anomalously low 5/7 values.

These lithologic, petrochemical, and desert varnish controlled spectral responses lead to characteristic TM band relationships which tend to correlate with conventionally mappable geologic formations. The concept of a Rock-Varnish Index (RVI) is introduced to help distinguish rocks with potentially detectable varnish. Felsic rocks have a high RVI, and those with extensive desert varnish behave differently, spectrally, from those without extensive varnish. The spectrally distinctive volcanic formations at Stonewall Mountain provide excellent statistical class segregation on supervised classification images. A binary decision rule flow-diagram is presented to aid TM imagery analysis over volcanic terrane in semi-arid environments.

INTRODUCTION

The Mackay School of Mines was awarded a 3-year contract in 1984 by NASA to investigate thematic mapper (TM) imagery over Tertiary volcanic centers in southern Nevada. The primary objective of the study is to establish relationships between cover types, chiefly secondary mineral coatings and primary lithologies, and to evaluate various cover-type contributions to the overall spectral composition in order to improve application of TM imagery to volcanic rock assemblages in arid to semi-arid environments. Three study sites in southern Nevada were

selected and 512x512 TM subscenes lifted for detailed examination over each. This paper will focus on the spectral character of the various volcanic rock assemblages and describe potentially useful image criteria for volcanic lithology discrimination and desert varnish evaluation.

Late summer to fall Landsat 5 TM scenes were read onto disk and all processing conducted on the Mackay School of Mines' VAX 11/780 based ESL compact interactive digital image manipulation system (IDIMS). Spatz, Taranik, and Hsu (1987a and 1987b)) describe preliminary image processing and lithologic discrimination techniques at these sites. TM imagery influence and origin of desert varnish were described by Spatz, Taranik, and Hsu, as well (1987c). Exceptional lithologic discrimination was achieved by longer wavelength band and band ratio composites and ISH and principle components transformations with emphasis on bands 3, 5, and 7.

STUDY SITES

The 3 study sites (Figure 1) provide superior settings in terms of exposure, preservation, lithologic diversity, and a preexisting data base collected by previous researchers at Mackay, principally Dr. Donald C. Noble. Each site centers on or straddles a well defined youthful caldera structure with discrete ash flow tuff deposits and associated lavas. Each center was source for multiple outflow ash deposits that extend over 30 km distally. Some of these major pyroclastic sheets are distinctive chemically. Devitrification, vapor-phase alteration, and welding history vary from unit to unit and within units. Rainfall averages 4-8 inches annually and vegetative cover is generally sparse.

The Stonewall Mountain project boundary straddles the eastern margin of the Stonewall Mountain caldera and the western margin of the Mount Helen caldera. Both Stonewall and Black Mountain lie within the Nellis Air Force Base Bombing Range in Nye County about 25 miles SE of Goldfield. Access is preceeded by security clearance with the Range Commander at Nellis in Las Vegas and military escort is required on range. Topographic relief within the Stonewall site varies mostly within a range of abount 600 feet. Elevation at Black Mountain ranges from about 6000 feet to 7235 feet and about 3200-6200 at Kane Springs Wash.

METHOD OF INVESTIGATION

Work conducted for this paper included imagery

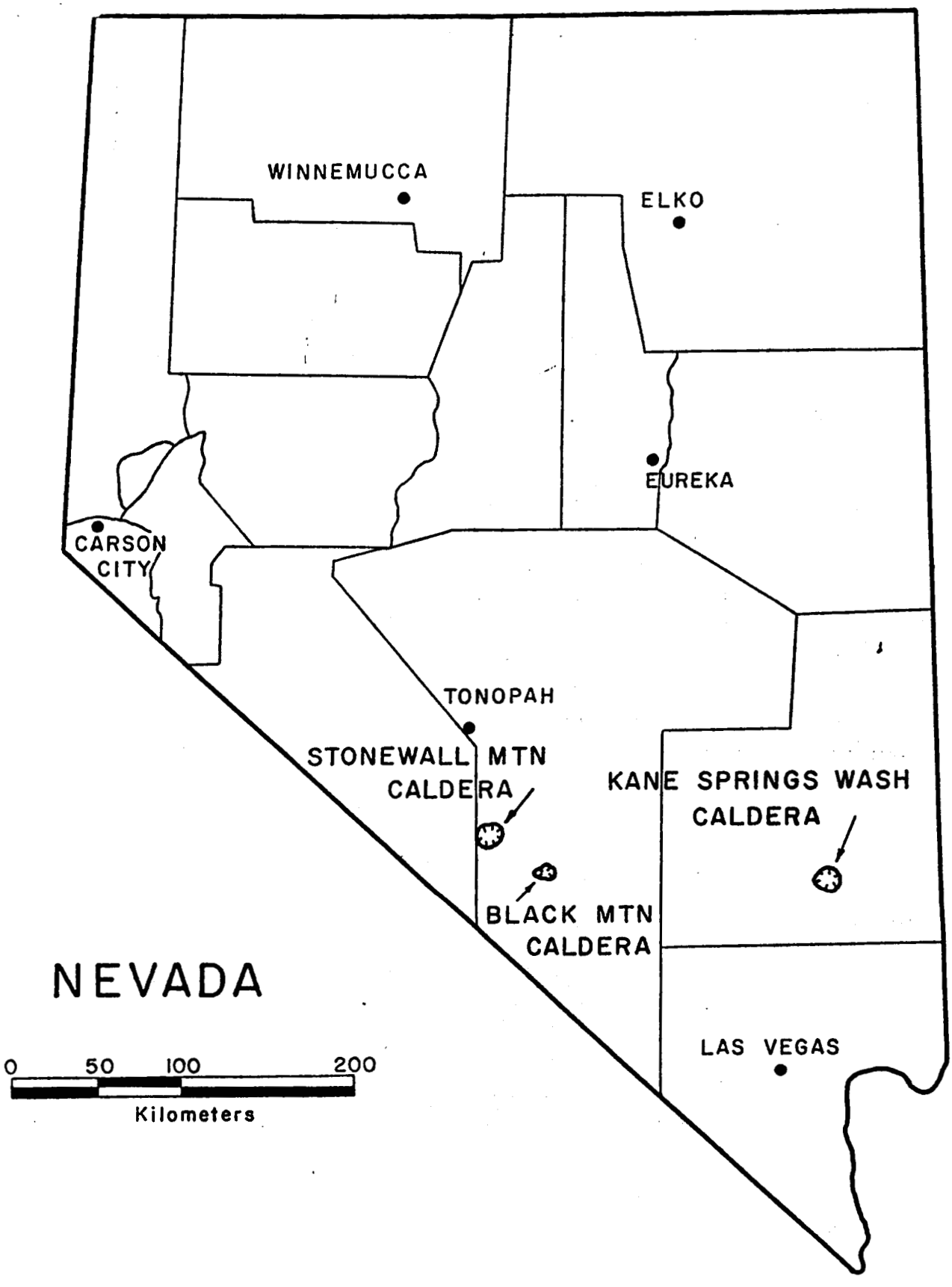

LOCATION OF LANDSAT TM TEST SITES

FIGURE 1. Location map of the project areas

ORIGINAL PAGE IS
OF POOR QUALITY

classification, both supervised and unsupervised; directional filters for basal glass enhancement; vegetation reduction, involving band ratios and band ratio addition and subtraction, at Kane Springs Wash; binary and ternary diagrams that plot volcanic units on band vs band and band vs composiiton axes; derivation of a Rock-Varnish Index (RVI); and development of a binary decision rule flow-diagram for assessment of volcanic caldera lithologies in arid to semi-arid environments. Other work, conducted last summer or during previous semesters, is reiterated for background. Geochemical analyses were contracted out and include results collected both during this investigation and analyses provided by Dr.Noble from earlier work on these volcanic centers.

IMAGERY PROCESSING

Imagery processing was accomplished on the School's Vax 11/780 based Electromagnetic Systems Laboratories (ESL, a subsidiary of TRW Inc.) compact Interactive Digital Image Manipulation System (IDIMS) and a compact personal computer image analysis station (Table 2). The compact IDIMS offers over 250 applications functions implemented by command language or menu.

Prior to conducting any field work and in advance of any significant knowledge of the areas under investigation, image processing was conducted on each of the 512 x 512 subscenes. This a-priori approach was intended to result in unbiased remote sensing units by objective processors. Field sampling was then partially based on these pre-field images, sample sites selected to include remote sensing units distinctive in terms of color, tonal, textural, or pattern characteristics. Further imagery processing was then conducted in the fall of 1986, after the previous summer's field work. The aim of subsequent imagery manipulation and assessment has been to refine enhancement techniques and contrast between rock units with benefit of direct field experience.

For each subscene the following images were produced and photographed with the system's Dunn camera peripheral on 35mm film:

INDIVIDUAL BANDS: 1,2,3,4,5,7
BAND RATIOS: 4/3, 3/1 or 3/2, 5/1 or 5/2, 5/7
SIMPLE COMPOSITES: 3-2-1, 3-5-7, 1-3-5, 3/1-5/7-4
ISH: individual intensity(I), saturation(S), hue(H)
on bands 3-5-7 and 1-3-5
ISH COMPOSITES: 3-5-7, 1-3-5, 1-2-4, 2-4-5
PRINCIPLE COMPONENTS: individual PC's 1,2,3,4,5,&6

ORIGINAL PAGE IS
OF POOR QUALITY

COMPOSITE PC's: 1-2-3, 2-3-4, 1-2-4, 1-2-5, 2-4-5
COMPLEX COMPOSITES: 3-5or7-I,S,or H (1-2-4);
3/1-7-I,S,or H (2-4-5);
3/1-5/7-I,S,or H (2-4-5);
3or3/1, 5or5/7, PC1or2;

Although image composites other than those listed above were reviewed, these band relationships and imagery renditions are thought to represent best contrast relationships between lithologies and should enhance coating characteristics inasmuch as emphasis is placed on the "alteration" bands, bands 3 and 7. Band 5 is a well established high contrast spectral interval for most cover types, especially lithologies with regard to divalent iron content. Each individual band image and composite was contrast stretched, linearly, using the IDIMS scaling function (described below) at a .5 truncation. All composites were color encoded red, green, blue (left to right). Some of the more effective images were edge enhanced by a kernel convolution technique described below.

The following list provides a brief description of the IDIMS functions utilized for this project and should help clarify captions on images presented in following sections. Discussions of image enhancement techniques have been presented by Taranik (1978b) and Sabins (1987).

SCALE. Each band was linearly stretched using IDIMS function "scale". Whereby an arbitrary amount of both the high and low tails of the brightness range distribution of pixels for each band is assigned to the maximum and minimum values respectively, and remaining intensity values stretched throughout the complete scale of 256. For final computation a histogram is calculated by the function. Experimentation yielded a consistently attractive value for truncation of 0.5 for most image manipulation applications. For principle component analysis, however, a truncation value of 0.2 proved superior. The result is a contrast enhanced image with brightness values extending the entire range of system resolution capacity, thus providing maximum brightness contrast between cover types.

RATIOS. Band ratios (Band x/Band y) are computed through IDIMS function "divide" and involve dividing pixel intensity values in the numerator band by corresponding pixel intensity values for the band in the denominator. Resulting values tend to smooth out topographic reflectance and provide relative brightness values representative of cover type.

EDGE. Edge enhancement techniques involve either coarse

ORIGINAL PAGE IS
OF POOR QUALITY

or fine scale adjustments to smooth out contrast variations or sharpen them. For our purposes, the edge enhancement function sharpens remote sensing units by increasing the contrast at unit boundaries. A "kernel" is produced by IDIMS function "KERNEL" whereby a 3 x 3 pixel size area was selected and an algorithm applied to each pixel at its center throughout the scene. The algorithm involves comparing the central pixel to brightness values of the surrounding pixels to identify those with a relatively large difference. Those central pixels whose intensities do vary markedly from the average of those surrounding it are either increased or decreased in value as appropriate to increase even further the intensity difference. The kernel is moved over each pixel by the function "CONVOL". The result is to enhance the edges of imagery units relative to bordering units thereby sharpening the contrast.

ISH. The ISH transformation is a commonly applied computerized image manipulation technique which subdivides colors in color composite images into the optical parameters - intensity (i), saturation (s), and hue (h) (Buchanan, 1979; Haydn, et.al., 1982). Red, green, and blue are transformed to intensity, saturation, and hue, and resulting 3 image composites thus represent I, S, and H, rather than the individual input bands. (There are 3 input bands.) The IDIMS function ISH applied throuout this project plots the three primary colors at the vertices of an equilateral triangle. Intensity is defined as the average of the intensities of each color (each of the original bands). Saturation indicates the purity of a color with respect to departure from achromatic (white) which plots at the center of the triangle. Saturation would thus be at a minimum at the center, a maximum on the triangle periphery. Hue is defined in relation to color. It begins at red (minimum), increasing toward green and then blue, and up to a maximum at red again. Each parameter - I, S, and H - range from 0-255. An RGB function IDIMS converts ISH to red, green, blue.

PRINCIPLE COMPONENTS. Descriptions of principle components statistical analysis (PC's) are given by Davis (1973) and Joreskog, et.al. (1976). Application to remote sensing imagery transformation has been described by Fontanel, et.al. (1975); Podwysocki, et.al. (1977); and Taranik (1978). PC's, the basis of modern factor analysis schemes, are the eginvectors of a variance-covariance matrix. The variance of two variables, in this case intensity values of two bands, is ploted on an x-y coordinate system. A point is then located perpendicular from each coordinate at the variance value extending a distance equal to the covariance. An ellipse is plotted with its center at the coordinate origin and bound near one

end by the two points. The vector from origin to the apex of the ellipse is PC1 and all intensity values are regressed to that vector. PC2 is perpendicular to PC1, extends through the coordinate origin, and is bound by the ellipse. It is always much shorter than PC1 and resultant intensity values considerably lower. Podwysocki (1977) describes resultant values as "new variables (components) which are linear combinations of the original variables; each component contains uncorrelated information". All six TM bands may be entered and a complex principle components analysis computed, resulting in 6 PC's. The IDIMS function KLTRANS takes a covariance matrix computed through function ISOCLS and computes PC's. The principle components transformation typically provides maximum contrast between cover types and PC composites aid distinction between lithologies, vegetation, and topographic effects.

OTHER. Functions used to classify imagery are described in some detail in the following sections which address both supervised and unsupervised classification.

GEOLOGIC SETTINGS

STONEWALL MOUNTAIN AREA

The study area at Stonewall Mountain involves two caldera structures - Stonewall and the Mount Helen calderas (Figure 2). The Landsat work scene selected for this site overlaps both. The erruptive event at Stonewall was young relative to the southern Nevada volcanic field in general - 6 to 6.3 m.y.a. (Noble, et.al, 1984) and involved a two component outflow ash sheet. Extracaldera outflow deposits from the Stonewall Mountain caldera - The Stonewall Mountain Tuff - consists of a lower pumice rich ash flow deposit - The Spearhead Member - overlain by a thiner, typically more densely welded ash flow sheet - The Civet Cat Canyon. The Civet Cat Canyon Member underwent auto-oxidation resulting in a distinctive deep reddish maroon brown color which forms a chocolate brown supergene coating.

A felsic suite of tuff and lava ranging in composition from rhyolitic to intermediate probably originated from the Mount Helen caldera. The units are cream to pale yellow in weathered outcrop. In places these felsic volcanics overly more mafic volcanics and fine airfall tuff. They appear to interfinger with the Stonewall Mountain Tuff. Basalt flows are present at two isolated locals within the work area. The western margin of the Mount Helen caldera is delineated by a normal fault conspicuous on Landsat images. The fault is bound on the west by quartzite pebble/cobble gravels,

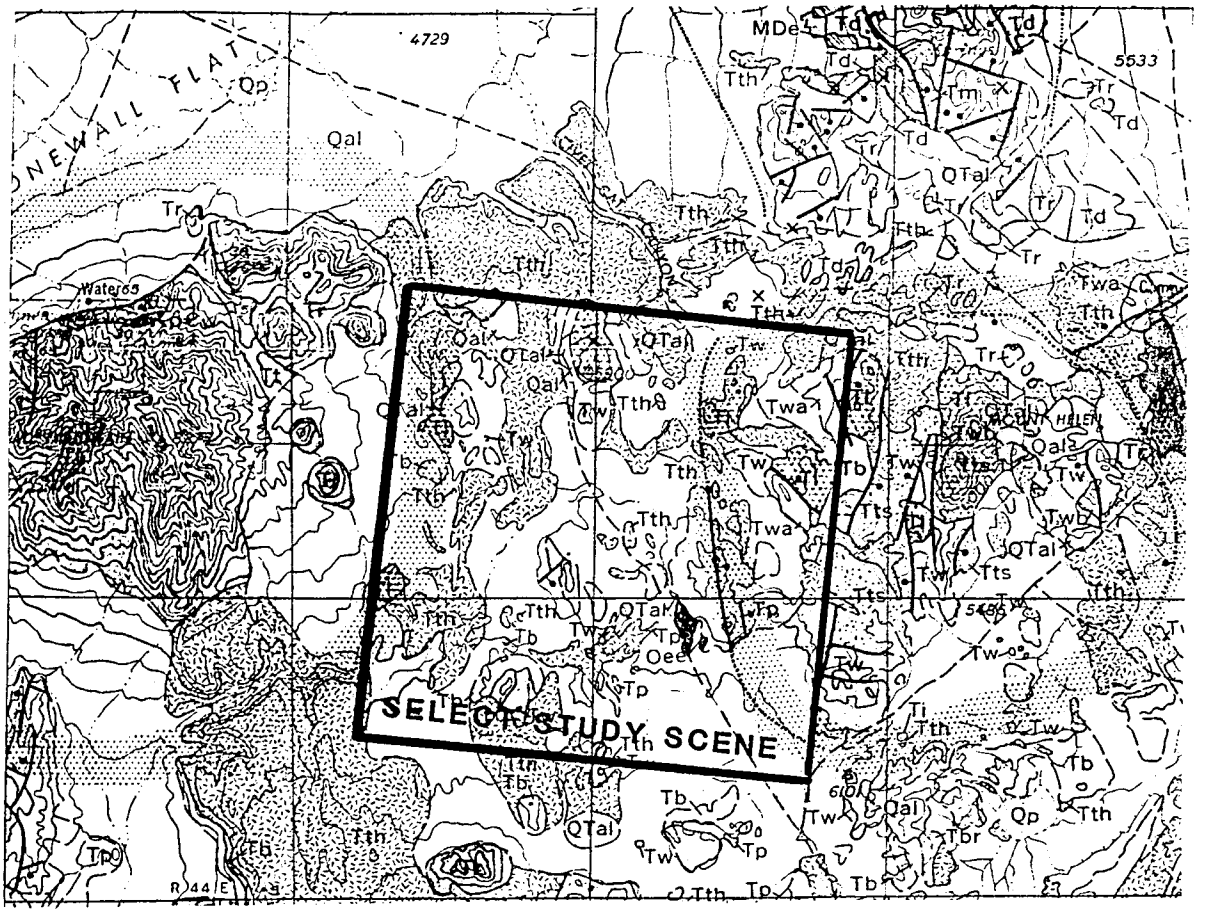

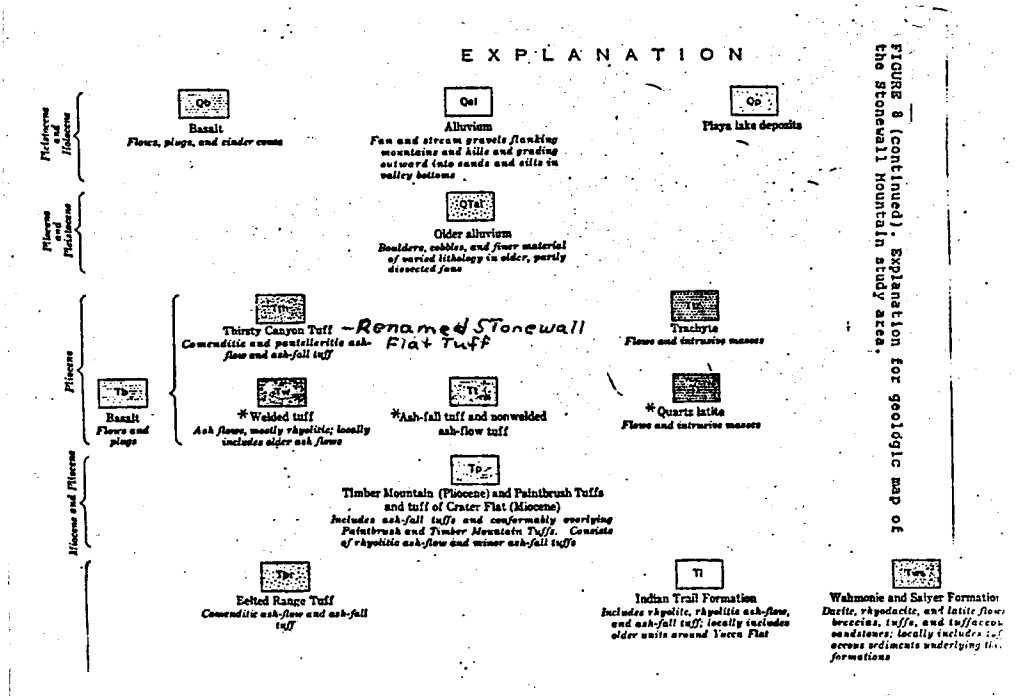

Figure 2. Geologic map of the Stonewall Mountain site (Copy of portion of Nevada Bureau of Mines Nye co. map)

ORIGINAL PAGE IS
OF POOR QUALITY

and on the east by felsic Mount Helen flows.

BLACK MOUNTAIN CALDERA

The Black Mountain study site consists of a concise well exposed, relatively small caldera complex (Figure 3). The geology was described by Noble, et.al.(1964 and 1984), and Noble and Christiansen (1974). Volcanic units are more numerous and diverse than at the Stonewall study area and were apparently produced in part by a multi-collapse sequence. The center is believed to have been active between about 6.5 to 8.5 m.y. ago. The Black Mountain volcanics consist of intracaldera lavas and an outflow sequence - The Thirsty Canyon Tuff (Noble, et.al, 1964). Basically 3 or 4 collapse events have been recognized, each preceded by subalkaline to peralkaline lava extrusion. Collapse was attended by major ash flow eruptions, alternating initially between subalkaline to comenditic compositions with a general trend toward greater peralkalinity upsection.

The Gold Flat member is the youngest ash flow deposit. It postdates final caldera collapse and is a pantellerite by composition (Noble, 1965). The unit is a highly evolved peralkaline end member with greater than 4% iron content. The final event at Black Mountain was central volcano fill by mafic trachyte lavas with peralkline affinities. The Labyrinth Canyon ash flow deposit which occurs in an isolated intracaldera patch on the west flank of the volcano was later recongnized by geochemical deduction (Noble, et.al., 1984) as distal Spearhead Member of the Stonewall Mountain Tuff.

KANE SPRINGS WASH

The Kane Springs Wash volcanic center was first described by Cook (1966) and Noble (1968). Detailed mapping and geochemical studies were conducted by Novak (1984 and 1985). Figure 4 from Novak (1984) shows area geology.

The center consists of a well defined central caldera collapse structure with a complex sequence of diverse intracaldera lavas, tuffs, and flow dome deposits that straddle the collapse event in time. The outflow formation consists of at least 8 distinct ash flow sheets, ranging in composition from subalkaline to peralkaline rhyolite with a pantelleritic trend.

The caldera rim fault is quite pronounced on the west and south edge of the caldera and marks a striking contrast

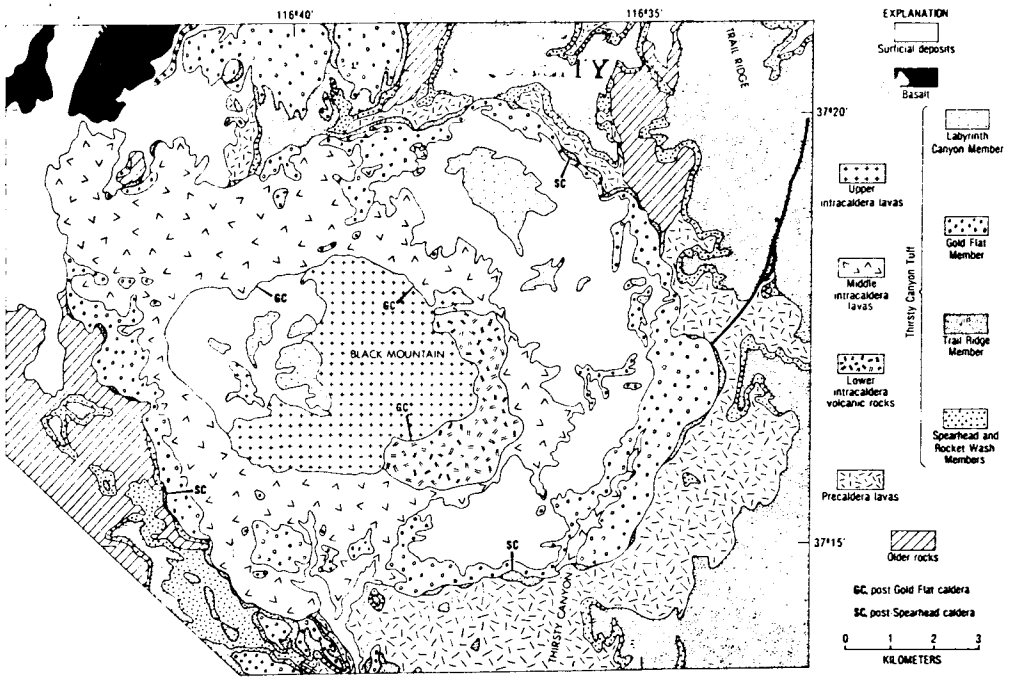

Figure 6. Geologic map of the Black Mountain caldera area, southern Nevada (compiled from Christiansen and Noble, 1968; Noble and Christiansen, 1968; O'Connor and others, 1966; and unpublished mapping by R. L. Christiansen and D. C. Noble).

Figure 3. Geologic map of the Black Mountain caldera (From Christiansen, 1979, compiled from work by Noble, Christiansen, and O'Connor.)

ORIGINAL PAGE IS
OF POOR QUALITY

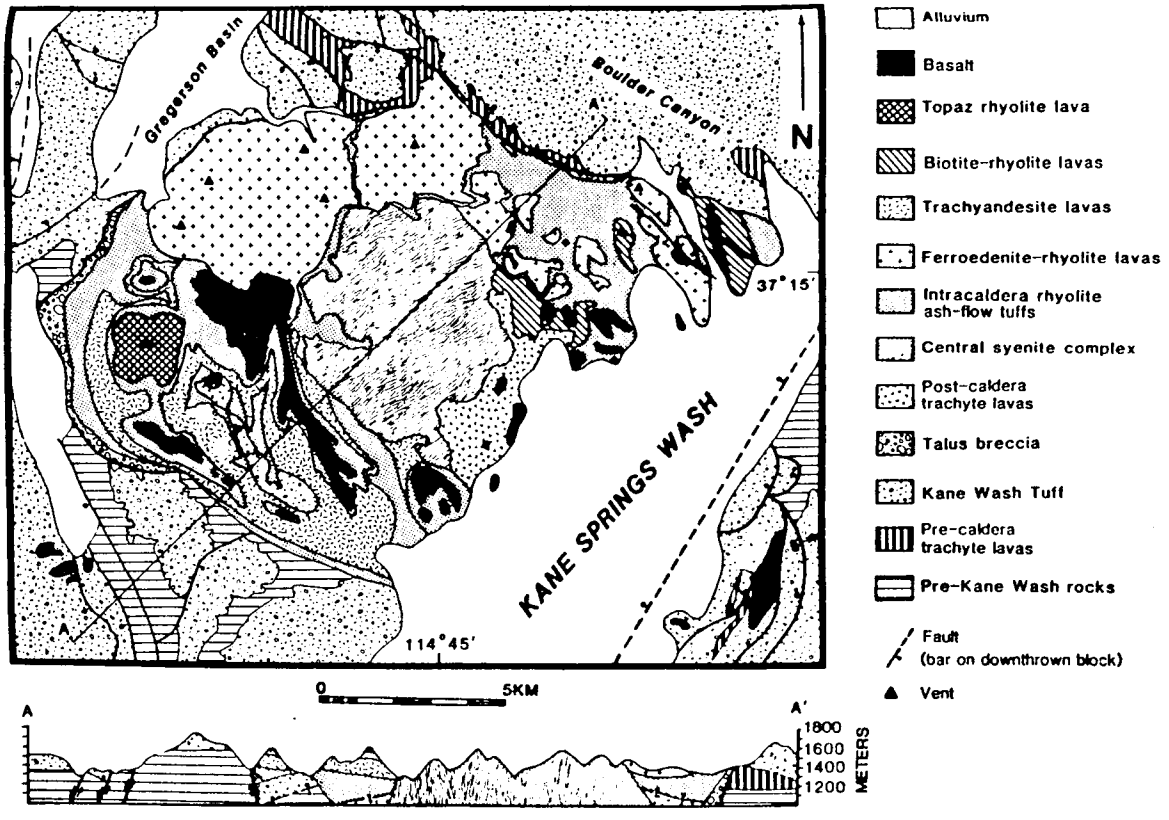

Figure 4. Geologic map of the Kane Springs Wash area (From Novak, 1984)

between intracaldera lithologies and outflow deposits. Intracaldera deposits consist of dark trachyandesite flows primarily overlain by white pumice-rich air fall tuff. Late basalt caps the intracaldera mesas. Intrusive through this sequence are flow dome complexes of topaz bearing rhyolite. In the NE portion of the caldera is a sequence of complexly emplaced silica poor tuffs and syenite domes introduced late in the depositional history, but which do not appear to have caused resurgent doming. The outflow sheets are ash flows with typical welding, vapor phase, and vitric zonal relationships. Some air fall tuff has been recognized interstratified between ash flow formation.

DESERT VARNISH

Early attempts to describe mineral coatings in desert environments (chiefly desert varnish) in a comprehensive fashion were published by White (1924), Laudermilk (1931), and Engel and Sharp (1958). A more quantitative approach to the study of coatings began in the mid-1970's and numerous workers have published their results since. Dorn and Oberlander (1981) in a fairly lengthy treatise on the topic do an excellent job of summarizing work on coatings up to that time.

Desert varnish is usually defined as the arid secondary phase at the weathered surface of rocks in arid to semi-arid environments. To most field geologists in the U.S. desert varnish is that conspicuous dark rusty brown to shiny black stain that commonly coats prominent bluffs in our semi-arid Southwest. Iron and manganese oxides are the distinctive components. For purposes of remote sensing, we are concerned with the entire surface of a rock exposure, which may include both true desert varnish, subvarnish alteration zones, and relatively fresh rock. Any given scene typically contains a combination of rock surface types. Previous workers have diverged on source of varnish constituents. Engle and Sharp (1958) concluded that the components of desert varnish are derived from the underlying host rock, whereas Dorn and Oberlander (1981) state flatly that the constituents are derived from external sources. The proponents of an external source point to wind blown dust as the feedstock.

We have investigated coatings from over 100 samples from the 3 project sites. Methods of investigation have included optical thin section observation, X-ray powder diffraction, IR spectrophotometry, ICP analyses, visible and near-IR spectrophotometry, gray level density slicing, and SEM scans with EDXA capability. Coatings are characteristically thin and discontiuous. They are a reddish brown to dark

brown amorphous mass that tends to coat mineral grains at the surface and penetrate as a thin film intergranularly up to 1-1.5mm into the rock. SEM scans reveal that the thickest surface deposits rarely exceed 20-30 micrometers and that even a well coated surface is dominated by much thinner films. The thick, 20-30 micrometer accumulations are sporadic and discontinuous, concentrated largely in minute protected recesses.

Major element compositions (SEM analyses) of coatings from rock surfaces of all rock types from each area, including quartzite from Stonewall Mountain, are quite similar - about 45-60% Fe and Mn and 40-50% Si and Al - an observation important to remote sensing efforts. Either Mn or Fe alone can exceed 30%. Except for Fe/Mn ratios on basaltic rocks tending to be higher than on other units, there does not appear to be any distinctive correlation between coating compositions and host rock lithology. No significant amount of clay minerals or other crystaline compounds have yet been detected, either from thin section observation, X-ray powder diffraction, or IR spectral scans. (Detail on compositions, distributions, and relationship of coatings to underlying rock is the subject of a paper in preparation by the authors and Jim Sjoberg of the U.S.Bureau of Mnes).

Coatings develop to an advanced stage of maturity only where the surface is resistant and durable. Surfaces do not exhibit significant coating continuity. Where coated surfaces become breached by weathering or where deposits have not matured to an advanced state, relatively fresh rock is exposed. Over any given surface about 4x4 meters or so square, significant varnish rarely accounts for over 50% of the exposure. Removal of coated surfaces is expedited by development of weathering rinds, .25-2.0 cm thick, which spall off outcrop surfaces. It is this process that leads to case hardening and exfoliation.

Penetration of electromagnetic energy within the TM range was studied by Buckingham and Sommer (1983) who found that maximum penetration for pulverized samples of clay minerals was about 50 micrometers. A mixture of goethite and kaolinite - 75/25 - stopped penetration of 0.8 - 1.0 micrometer wavelengths at around 25-30 micrometers. Amorphous, translucent compounds like those that make up the coatings of this study would transmit light further than crystaline mixtures of iron oxide and clays. In other words, light would penetrate in part (increasingly with increasing wavelengths) completely through even the thickest concentrations of coatings yet discovered in this study reflecting to at least some degree the primary character of underlying rock to the extent that it is unaltered.

IMAGERY CHARACTERISTICS

Imagery processing methods were described above. Landsat 5 Thematic Mapper data, bands 1, 2, 3, 4, 5, and 7, were investigated for this study. A multivariate statistical evaluation of pixel values for each scene was conducted with IDIMS function ISOCLS. A mean and standard deviation for each band and covariance matrix between bands were computed. Correlation coefficients between bands were derived by dividing covariance by the product of standard deviations of respective bands. The principle components transformation utilizes variance and covariance statistics, resulting in eginvectors. Eginvalues are a measure of the amount of variance contained in each PC. In general PC2 contains rock/soil dominated variance, and PC3 variance is dominated largely by vegetation.

In this section imagery characteristics of each major volcanic unit at each of the 3 study sites is discussed with a view toward establishing effective imagey correlation and image combinations for formation discrimination and mapping. In all color composites, the encoded color sequence is red-green-blue (RGB). Studies so far indicate vegetation (only 25-30% of surface cover) is unimportant as a significant spectral control in the images at Stonewall.

STONEWALL MOUNTAIN AREA

SPEARHEAD TUFF. The Spearhead Tuff exhibits little spectral variation throughout the visible and near-IR. It is relatively dark in all TM bands in contrast to surrounding alluvium and Antelope Springs rhyolits. Reflectivity decreases slightly and the unit darkens subtly in band 5 relative to adjacent cover in the scene. Darker trends tend to increase the tonal contrast somewhat in 5/7 images. Intensity increases slightly in 5/2 images. These band relationships, of course, control color characteristics in false color composite images. So in 3/1-5/7-4 images, encoded RGB, the unit is magenta indicating higher reflectance in the 3/1 and 4 images with low reflectance in 5/7, and the unit is blueish gray in the 3-5-7 image due to higher reflectance in bands 3 and 7. In individual principle component images, the unit is brightest in PC3 with high brightness also in PC2 and PC4. Thus in the 3/1-5/7-PC2 composite the unit is a fairly distinctive dark purple. ISH computation on bands 3-5-7 result in indistinct low contrast tones over the unit in the saturation and hue modes, darker though in the intensity image. This results in a distinctive dull army

green hue in the ISH composite. Indeed, basalt exposures, shadows, and the ash flow units with their dark desert varnish coatings tend to register high DN values in the saturation mode. Relationships are similar on ISH images of bands 1-2-4, thus a hue composite of bands 1-2-4 with scaled bands 3 and 7 results in distinctive blueish hues over the unit; green if intensity is used instead of hue in the same configuration.

CIVET CAT CANYON TUFF. Reflectance over Civet Cat is low in all bands over the main Civet Cat Canyon flow; however, the the spectrally distinctive Civet Cat Canyon cap rock, reflectance is relatively low in bands 1, 2, and 3 and high in bands 4, 5, and 7, increasingly so in the later 3 relative to other cover in the scene. These spectral relationships cause the cap rock zone to be subdued in 3/2 and 5/7 ratio images, but strikingly bright in the 5/2 image. High scene reflectance in band 7 creates high contrast turquoise blue over the unit in 3-5-7 images. The unit registers a dull, indistinct pale grayish green in the 3/1-5/7-4 image. There is a low intensity but high saturation and hue response for the cap rock in ISH computations with bands 3-5-7, resulting in a distinctive moss green contrast in the composite ISH image. On ISH images with bands 1-2-4 the unit shows low values in intensity and hue, high values in saturation, but low contrast in all three modes. Civet Cat is strikingly bright in PC2 images, growing somewhat less so in PC's 3 and 4. This results in impressive discrimination capacity over the unit in the PC2-PC3-PC4 and PC2-PC4-PC5 images. The unit is also rather anomalous on some of the more exotic composites, including especially the 1-4-Hue image, Hue computed on bands 3-5-7; the 3/1-5/7-PC2 image, and a 3-7-Hue (bands 1-2-4) composite. A 3/1-PC2-Hue (bands 3-5-7) is especially effective in highlighting the Stonewall Flat Tuff in general.

ANTELOPE SPRINGS RHYOLITE. Antelope Springs consists of a lower reddish, ferruginous rhyolite and a more alkaline highly reflectant upper deposit. Some of the formation appears intrusive, and hydrothermal alteration consisting of hydrous secondary minerals occures in places. The lower unit is relatively dark in all bands, but distinctive in many of the false color composites. The upper unit exhibits high reflectivity in all bands with deminishing intensity in longer wavelength bands 5 and 7. Band ratios for the high albedo upper member tend to dampen intensities relative to other cover and enhance differences in iron oxide coatings and clay altered surfaces in certain locations. For example, several exposures are quite bright in 5/7 ratio images. The unit contrasts markedly with other formations in most color composite images. On 3-5-7 and

3/1-5/7-4 images the upper unit is cream colored with iron oxide stained areas light reddish to red brown over the lower member. On the ISH computations, bands 3-5-7, the upper unit is bright in saturation and intensity, light to medium gray in hue. In 1-2-4 ISH renditions the deposit is quite dark in hue and saturation, light in the intensity mode. These felsic rocks respond with bright intensity in PC1 for the upper member, dark for the lower. The upper unit is dark and indistinct in PC2, and with only slight variation in higher PC's. Thus PC1 overpowers other bands in composites in which it is included and PC composites without PC1 tend to obscure the upper member. In the 3/1-5/7-PC2 image the light colored upper unit is brighty yellow to reddish and quite conspicuous. Perhaps the greatest overall contrast over the unit is exhibited by the 3-7-Hue (bands 1-2-4) image in which it is highlighted in bright yellow and the 3-5-7 ISH composite in which it is bright red.

BASALT. Basalt is dark in all bands, decreasing slightly in brightness in longer wavelength bands 5 and 7 relative to adjacent cover possibly due to the greater depth of penetration of the lower energy radiation and greater contribution of lithology, relative to desert varnish, to the spectra. It is thus medium gray and obscure in the 5/7 image and not appreciably changed by 3/2 and 5/2 ratios. On the 3/1-5/7-4 composite basalt is swamp green and well highlighted. It is dark brown on the 3-5-7 composite. In individual band modes of the 3-5-7 ISH transformation, the unit is dark. In 1-2-4 ISH, saturation and hue images it is very bright. Thus on the 3-7-Hue (bands 1-2-4) composite basalt is purple and on the 3-5-7 ISH composite, greenish. It is very dark in PC1, obscure and indistinguishable in PC2, slightly brighter in PC's 3 and 4. It is highlighted, therefore, by blue in the PC1 PC2 PC4 composite, but cannot be discriminated on the PC2 PC4 PC5 image. On the 3/1-5/7-PC2 image the unit is dark green.

BLACK MOUNTAIN CALDERA

Imagery over the Black Mountain study area differs from that of the Stonewall area primarily as a result of more diverse vegetative cover. Lithologies are more varied as well. Still the outflow sheets tend to be readily mappable with Landsat TM imagery. Vegetation has been described above and the 4/3 ratio image highlights zones with relatively heavy growth. This image is matched very closely by the PC3 image which also presents vegetation in strikingly bright contrast.

OLDER LAVAS AND TUFFS. The older felsic lavas and tuffs

are the most reflectant cover in lower wavelenght bands, 1-4. They are intermediate in reflectance at higher wavelengths. In the ratioed images the unit tends to be dull, intermediate in intensity and indistinct. Some areas over the unit, however, exhibit a brighter signature in the 3/2 image probably due to iron oxide staining observed inthe field. Alluvial material and drainages down slope of these areas are also bright. The deposit is a distinctive rusty cream color on the 3-5-7 composite. It is bright on both the PC1 and PC2 images and therefore exhibits a yellow signature on composites combining PC's 1 and 2, or a reddish color if only one of them is in combination with other variables and encoded red. In the 5-7-PC2 composite the unit is a pastel purple due to high DN values in 5 and PC2 and low DN values in band 7. With ISH transform on bands 3-5-7 the unit is quite bright in the intensity mode relative to other cover; bright in saturation; but only medium in hue. Thus a distinctive yellow hue manafests over these rocks in the 1-4-Hue composite. (The hue parameter is subdued for this formation.)

CRYSTAL RICH LAVAS. The inter-ash flow lava flows at Black Mountain, exclusive of Trachyte of Hidden Cliff, form a generally coherent remote sensing unit at Black Mountain. The lavas are dark in all bands, growing slightly darker with increasing wavelength. Lavas of Ribbon Cliff seem to be slightly darker than the others in bands 5 and 7. The units tend to be light to medium-light gray and indistinct in the ratio images. In the color composite 3/1-5/7-4 image the lavas are yellowish green and basically indistinguishable from Trachyte of Hidden Cliff. On the 3-5-7 image, however, they are a greenish brown. Lavas of Ribbon Cliff are more reddish than the other lavas on this image possibly reflecting a higher proportion of brighter superficial iron oxide staining. This distinction is mirrored on the 1-4-Hue (bands 3-5-7) image. On the 3-5-7 band ISH images, the lavas are dark in saturation and hue; indistinctive medium gray in the intensity mode. In the principle components transformation lavas are brightest relative to other cover in PC2 and PC4, dark in PC1. So in the PC composites, PC2 controls their contrast and in composite PC1 PC2 PC3 images they are greenish, and in PC2 PC3 PC4, reddish. They contrast in the later with Trachyte of Hidden Cliff which is emerald green probably due to the vegetative response of the summit area of Black Mountain.

TRAIL RIDGE TUFF. The Trail Ridge Tuff is essentially indistinguishable from Lavas of Pillar Springs, with which it is closely related both in time and space and in composition. The Pillar Springs Lava followed the Trail Ridge Tuff eruption to help form the classic volcanic

sequence for caldera volcanism of this type.

GOLD FLAT TUFF. The Gold Flat Tuff is an unusual rock petrochemically and is distinctive spectrally as well. This peralkaline deposit is very highly evolved magmatically and contains a high proportion of large ion lithopile elements and other incompatibles, including Ta, Rb, Th, and rare earths. Reflectance increases as wavelength increases to brightest in band 7. For this reason the unit is distinctly dark in the 5/7 image and reddish to magenta in 3/1-5/7-4 false color composites. The unusually high reflectance in band 7 relative to other scene cover gives rise to a strikingly bright turquoise blue hue in the 3-5-7 composite. Gold Flat Tuff is bright in PC1, very dark and anomalous in PC2, and dark as well in PC3 except over its northern exposures where it is masked by the bright response of vegetation. It is mediuim gray, indistinct in PC's 4,5 and 6. This relationship among eginvalues results in reddish hues over the formation in composites involving PC1 and bluish to purplish hues in the Pc2 PC3 PC4 composite. The unit is intensely bright in saturation and hue images with ISH transformation on bands 3-5-7; medium in intensity in the intensity mode. On the ISH false color composite Gold Flat Tuff is a very distinctive pale magenta. On the 5-7-PC2 composite, the formation is brilliant mustard yellow, but similar to Labyrinth Canyon Tuff. It is light purple in the 1-4-Hue (bands 3-5-7); blue where vegetation includes golden grasses and scattered low juniper.

TRACHYTE OF HIDDEN CLIFF. Mafic trachyte forms the central volcanic edifice and is very dark in all bands except 4 and 5 in which it is an indistinct contrast in medium gray. Spectral response appears to be influenced by vegetation, which in this case would be golden cheat grasses and lichen. The unit is very bright relative to other cover in 5/7 and 4/3 images, forming a slightly stripped pattern that apparently follows drainages and is probably caused by high vegetative reflectances in band 4. In individual PC's the deposit is quite dark in the first PC; very light due to vegetative interference in the third. Mafic trachyte is pinkish purple on the PC1 PC2 PC3 composite yellowish green in the PC2 PC3 PC4 rendition. It is indistinct from other lavas in the PC2 PC4 PC5 image. In the ISH transform of bands 3-5-7, the unit is very dark in intensity and hue; medium gray and indistinct in saturation. On the ISH composite it is purplish. In the 1-4-Hue (bands 3-5-7) image, mafic trachyte is dark forest green and a dull army green on the 3-5-hue (bands 1-2-4) image.

LABYRINTH CANYON TUFF. The Labyrinth Canyon ash flow

tuff, really a distal facies of Spearhead Tuff (Noble, et.al, 1984), is spectrally similar to but distinct from Gold Flat Tuff. It tends to be moderately to only slightly bright in bands 1-3, quite bright in bands 4 and 5; somewhat less so in band 7. It is slightly less reflectant in band 7 than Gold Flat Tuff which aids its descrimination in false color composite images which take this disparity into account. It is bright in the 3/2 image, possibly due to it's orangy buff color, and medium gray with 5/7 ratios, but much lighter in tone from the Gold Flat Tuff. Labyrinth Canyon is a pale powder blue and distinct from Gold Flat in the 3-5-7 composite and unique in color contrast as well in 3/1-5/7-4 hybrids in which it is a very pale pink. The unit is bright in PC1, dark in PC2. It appears masked by the bright vegetative response of cheat grass in PC3. It is pale pinkish lavender on the PC1 PC2 PC3 composite; a bright orangy red on the PC1 PC2 PC4 configuration. Saturation and hue images of bands 3-5-7 give the unit a very bright signature, less so in the intensity mode. The deposit occurs with fair color contrast as well in the 1-4-Hue (bands 3-5-7) and the 3-5-Hue (bands 1-2-4) composites. Color is not unique for the unit on the PC2 composites with bands 5 and 7 and bands 3 and 7.

KANE SPRINGS WASH VOLCANIC CENTER

Imagery response of units at Kane Springs Wash is influenced much more strongly by topography and vegetation than the other 2 study sites. Topographic relief is almost 1000 meters and juniper trees dot the mesa tops, particularly in the northern part of the caldera. Other vegetative cover is also thicker throughout the scene, including foxtail grass, cheat grass, atroplex, sage brush, boxbrush, and cactus plants.

HICO TUFF. The Hico Formation is the oldest unit in the scene. It is distinct chiefly due to image textural properties. On some images, particularly the Pc1 PC2 PC3 composite, alternating densely welded and vapor phase altered layering gives rise to red and white banding. Reflectance from Hico tuff increases in intensity in higher wavelength bands. The unit is bright in 3/2 and 5/2 ratio images, darker on a 5/7. It is indistinct in simple color composites and hybrid composites. The deposit is bright in PC1, obscure in other PC's. In the ISH transform, bands 3-5-7, the section is relatively bright in the intensity mode, medium gray in hue and saturation. Complex color composites tend to highlight the interval best. In PC1 PC2 PC3 and PC1 PC2 PC4 composites the formation is characterized by a reddish banded image. It forms a light powder blue in the 1-4-Intensity (ISH, bands 3-5-7) image

and exhibits a suble distinction in other ISH hybrids with other bands, for example, a 3-7-Saturation (bands 2-4-5). the 3-5-7 ISH Intensity parameter image exhibits the unit with relatively bright intensities.

KANE WASH TUFF (UNITS V1 AND V2). The Kane Wash tuffs exhibit medium gray tones in lower wavelength bands, but are relatively bright in band 5, increasing in intensity in band 7. The unit is quite bright in the 5/1 and 5/2 ratio images, rather dark in the 5/7 image. In the 3-5-7 composite the section is a distinctive powder blue. It is an indistinct red in the 3/1-5/7-4 image. The tuffs are extremely bright in the Hue mode of the 3-5-7 ISH transformation; dark in saturation; and medium gray in the intensity mode. Its a reasonably distinctive lavender in the ISH composite. In PC1 Kane Wash Tuff is medium gray; in PC2 quite dark where densely welded; then relatively light in PC's 3-5. In composite PC's - 1-2-3 and 2-3-4 - the formation is distinct, especially in the latter in which it tends toward bright blue. In more exotic renditions with ISH and simple band hybrids the section is typically highlighted with some characteristic tint. This appears to be due primarily to the presence of large areal exposures or platforms of densely welded zones.

AIR FALL TUFFS. The air fall tuffs which tend to be very light in color are highly reflective in all wavelengths. This characteristic controls this unit's response in false color composite images. These tuffs are quite bright in PC1, even brighter in PC2. Tonal contrast is obscure in higher PC's. In all ISH transformations these glassy beds are bright in intensity mode, obscure in saturation and hue. The deposits are more uniquely highlighted by PC composites and the 1-4-Saturation (bands 3-5-7) image.

SYENITE COMPLEX. The syenite complex is recognizable on images only as an anomalous textural pattern, involving tone and color variation throughout a roughly annular zone. The pattern is created by irregular reflectance properties over relatively small areas throughout the complex. Reflectance is variable, but more consistently bright in the higher wavelength bands. In individual PC images the unit exhibits overall medium intensity brightness except in PC2 in which it is relatively dark. The subtly distinct busy textural pattern seems fairly equally highlighted in complex composites with highly variable hues and tints. Two subcircular zones within the complex, exhibit relatively bright signatures similar on may images to the topaz rhyolite dome described below. These zones reflect syenitic flow dome complex within the syenite complex.

TRACHYANDESITE LAVAS. The trachyandesite lavas are

exposed primarily in the canyons within the caldera complex. They are thus largely obscured by shadows with which they tend to blend. The unit is relatively nonreflectant and dark in all bands. It is tonally light in the 5/7 image. The deposit is light in tone in PC2, dark in all other PC's. The formation is anomalously dark in the hue mode of the 3-5-7 ISH transform and bright in saturation. It is a reddish brown to greenish brown color in the 1-4-Hue (bands 3-5-7) image and the 1-4-Intensity composite.

RHYOLITE FLOW DOMES. The rhyolite flow domes and syenite domes of the syenite complex exhibit very similar imagery signatures. Rhyolite domes are characterized by peralkaline tendency and high F and Cl as well as other incompatible elements that partition into highly evolved magmatic differentiates. One characteristic of these units is a concise small subcircular outline. Tonal contrast and color patterns within these deposits is somewhat variable. In that regard, thus, they behave similarly to the syenite complex described above. The rhyolite and syenite flow domes are highly reflective in all bands, but the rhyolite domes more so in band 7. For that reason rhyolite domes form strikingly anomalous dark bullseye contrasts in the 5/7 ratio image. It is a brilliant red color in the 3/1-5/7-4 composite. The formation is uniquely bright in PC5, quite bright also in PC1. It is darker in PC2. The unit tends to resemble the Kane Wash Tuffs in many of the composite images. It exhibits slight deviation from the tuffs, however, in the 1-4-Saturation and Intensity (bands 3-5-7) composites. Perhaps the best images for its discrimination are the individual bands, PC5, 5/7 ratio, and saturation with bands 3-5-7, in which the unit appears dark.

LATE BASALT. Basalt caps the mesas within the caldera. It's spectra are contaminated by vegetative cover, including sparse to moderately dense juniper. The basalt flows are dark in all bands, with a slight increase in band. The unit is rather light, however, in the 5/7 ratio image and therefore greenish on the 3/1-5/7-4 composite. In the 3-5-7 composite the lavas are blue to greenish. The unit is very dark in PC1; indistinct in other PC's. On the PC composites, 1-2-3 and 2-3-4, basalt is dark blue to dusty blue. On the intensity image of the ISH function on bands 3-5-7 the formation is dark but indistinct in hue and saturation. On the 1-4-ISH composites the basalt is a dark felty green. The unit is a rather distinctive purple on the 3/1-5-PC2 image.

DIRECTIONAL FILTERS

Directional filters were applied to a Stonewall Mountain contrast enhanced band 5 image in an attempt to highlight thin airfall tuff deposits and basal vitropheres (Appendix A). Airfall tuffs (Plinian type) often preceed ash flow deposition, and basal vitropheres may form at the bases of ash flows where bedrock was cool. The occurrence of airfall tuff and basal vitrophyre is critical to formation discrimination and mapping of ash flow sections, for it is the lower contacts of these deposits that demark, by convention, the lower contact of individual formations.

Filters involve IDIMS functions KERNEL and CONVOL, which first create a mask or "kernel" and then "convolve" it to the image. The mask or kernel is a two dimensional matrix, in this case a 3 x 3 matrix which centers on each pixel in the scene and weights the surrounding pixels according to preset amounts. The sum of the new weighted values of surrounding pixels is then compared to a new weighted value for the central pixel. If the value of the central pixel is less than the summed value of surrounding pixels than the central pixel value is changed to the latter. For edge enhancement, the technique tends to sharpen borders between areas of gradational tonal contrast. For our purposes, that of highlighting linear contrast of basal glass and airfall, a directional bias (Jensen, 1986) was applied in order to take advantage of the general trend of ash flow deposits in the Stonewall scene.

Both southwest and northeast (Figure 5) filters were successful in enhancing basal airfall deposits. Airfall at the base of Spearhead Tuff is apparent in Figure 5 at "A" and at the base of Civet Cat Canyon Tuff at "B". the airfall deposit at the base of Spearhead is also manifest on normal nonedge enhanced images; however, the basal glass exhibited under Civet Cat Canyon Tuff was not observed in other images.

VEGETATION SCREENING

Vegetation forms only 20-40% of the cover at the Stonewall Mountain and Black Mountain study sites; however, at Kane Springs Wash, with scene relief of over 3000 feet and elevations above 6000 feet, shrub conifer add to the vegetation population in the northern portion of the area leading to significant spectral contamination from a lithologic point of view.

A preliminary attempt at image vegetation reduction was undertaken at Kane Springs Wash partly in anticipation of

ORIGINAL PAGE IS
OF POOR QUALITY

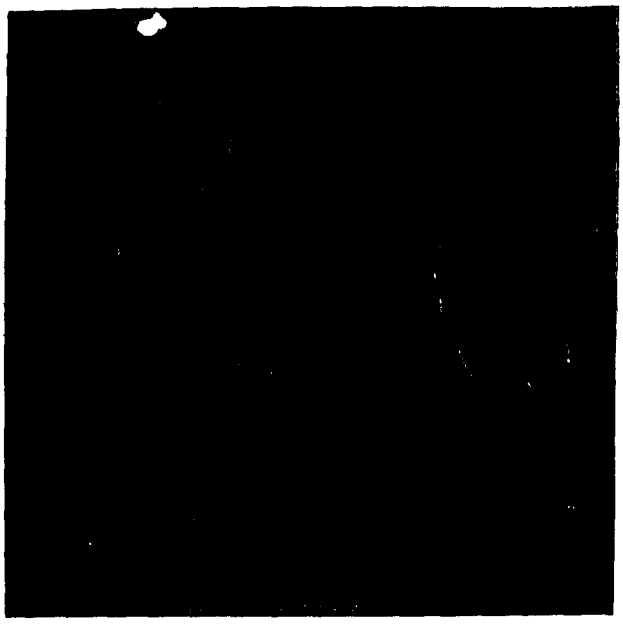

Figure 5. NE directional filter of band 5, Stonewall area, with a 0.4-1 add back. Note enhanced air fall ash layer at "A".

Figure 6. 5/4+4/3 image of Kane Springs Wash. This configuration tends to reduce vegetative interference.

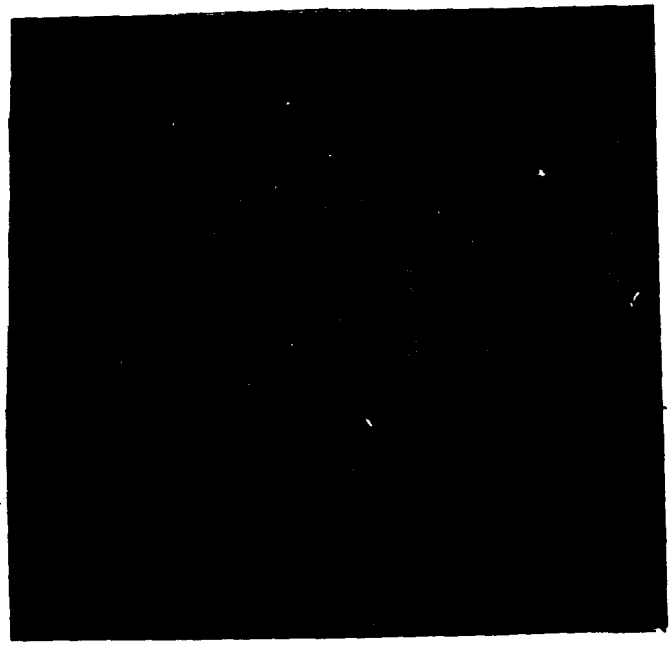

Figure 7. Unsupervised classification of the Stonewall scene (6 bands), using ISOCLS. Classes=16.

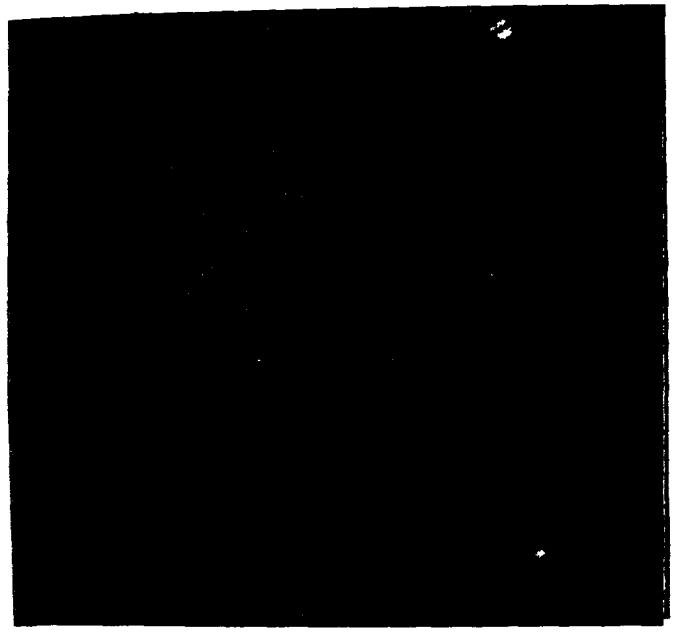

Figure 8. Unsupervised classification of the Kane Springs Wash site (6 bands), using ISOCLS. Classes=16

TIMS data acquisition over the area by NASA. Simple band ratios and many ratio subtraction and addition techniques were conducted (Appendix B). Since vegetation reflectance is higher than rock/soil in band 4, but similar in band 5, a 4/3+5/4 image (Figure 6) tends to smooth over vegetative response by adding back the vegetation enhancement of a 4/3 image to the dark mask over vegetation resulting in the 5/4 image. Other additive and subtractive combinations were attempted, including ratios 2/3, 4/3, 7/2, etcetera (Appendix B). A 5/2 4/3+5/4 7/2 color composite provides a vegetation reduced image, but in all of these attempts some vegetative response remained.

SPECTRAL CLASSIFICATION

UNSUPERVISED CLASSIFICATION

Unsupervised classification was performed on each of the 3 study sites, using IDIMS function ISOCLS (Appendix C). ISOCLS applies a clustering algogithm to a multispectral image, in this case, 6-banded images, in order to partition multivariate data points into disparate catagories with similar statistical properties. The function operates by "split" and "combine" iterations, involving the distance between data points and the cluster means. If a data point's standard deviation is greater than the default value of 4.5, "spliting" occures and a new cluster is created. The maximum number of clusters set was 16, the default value.

Comparison of Figures 7 and 8 with the corresponding geologic maps exhibited in Figures 2 and 3 seems to result in fairly weak lithologic correlation. Some units are fairly well represented, in part, by the classes designated by ISOCLS - some basalt at Kane Springs Wash and some of the Gold Flat tuff at Black Mountain, for example - but for the most part, spectra of the classified clusters include alluvium and mixed pixel zones with many discrepancies and only nominal lithologic correlation. The method seems to work best at the Stonewall Mountain area where vegetation and topographic relief provide least interference.

The unsupervised classification scheme at Stonewall Mountain was regrouped by function, RECLAS which reclasses pixels if they differ from pixels in a surrounding 3 x 3 matrix. The algorithm results in a reduction of classes and a more generalized classification which improves lithologic correlation somewhat.

SUPERVISED CLASSIFICATION

Supervised classification with IDIMS function CLASFY was applied at the Stonewall Mountain study site (Figure 9). The computer processing procedure involves definition of training sites (Functions TR and TA) on known cover types, in this case, volcanic formations (Figure 10); assigning the training sites to a special file (IRRECV) and performing statistical evaluation of the pixels within the training sites with the function, STATS. CLASFY then evaluates all pixels according to a maximum likelihood decision rule based on class covariance matrices and mean vectors (Jensen, 1986).

The supervised method resulted in generally positive classification of pixels according to lithology (Figures 11 and 12). Coherent groups of contiguous pixels correspond with mappable formations at a scale of about 1:50,000. Isolated pixels and narrow, dendritic, reticulate or erratic patterns do not typically reflect exposed or mappable bedrock. These pixels appear to be largely unusual alluvium or detritus without distinct classes of their own.

Function RECLAS was also applied to the supervised classification image at Stonewall, resulting in less erratic, outlying, pixels. This method leads to better overall groupings for geologic mapping purposes.

LAB SPECTRA

A few select samples of rock surfaces were scanned for visible/IR spectral characteristics on JPL's Beckman lab spectrophotometer last Spring (Figure 13). The results support band reflectance relationships exhibited in contrast enhanced single band images and hybrid composites involving band ratios. Of most significance:

1. Lower wavelength bands are more absorbent to surfaces with desert varnish (coated).
2. At higher wavelengths - bands 5 and 7 - varnish absorption becomes less significant since lower E radiation penetrates deeper.
3. The progressively decreasing influence of varnish absorbance at longer wavelengths causes lower 5/7 ratio values for surfaces with varnish.
4. As varnish cover increases 5/7 ratio values should decrease.
5. The slope of the reflectance curve for Gold Flat Tuff, a highly evolved unit with a high

ORIGINAL PAGE IS
OF POOR QUALITY

Figure 9. Supervised classification of the Stonewall area (6 bands), using CLASFY on 13 training sites.

Figure 10. The 13 training classes used for lithologic correlation for supervised classification.

Figure 11. Civet Cat Canyon cap rock (colored) isolated by TCC from the supervised classification scheme. three training sites shown.

Figure 12. Antelope Springs rhyolite. Lower member in orange, upper in yellow. isolated by TCC from the supervised classification.

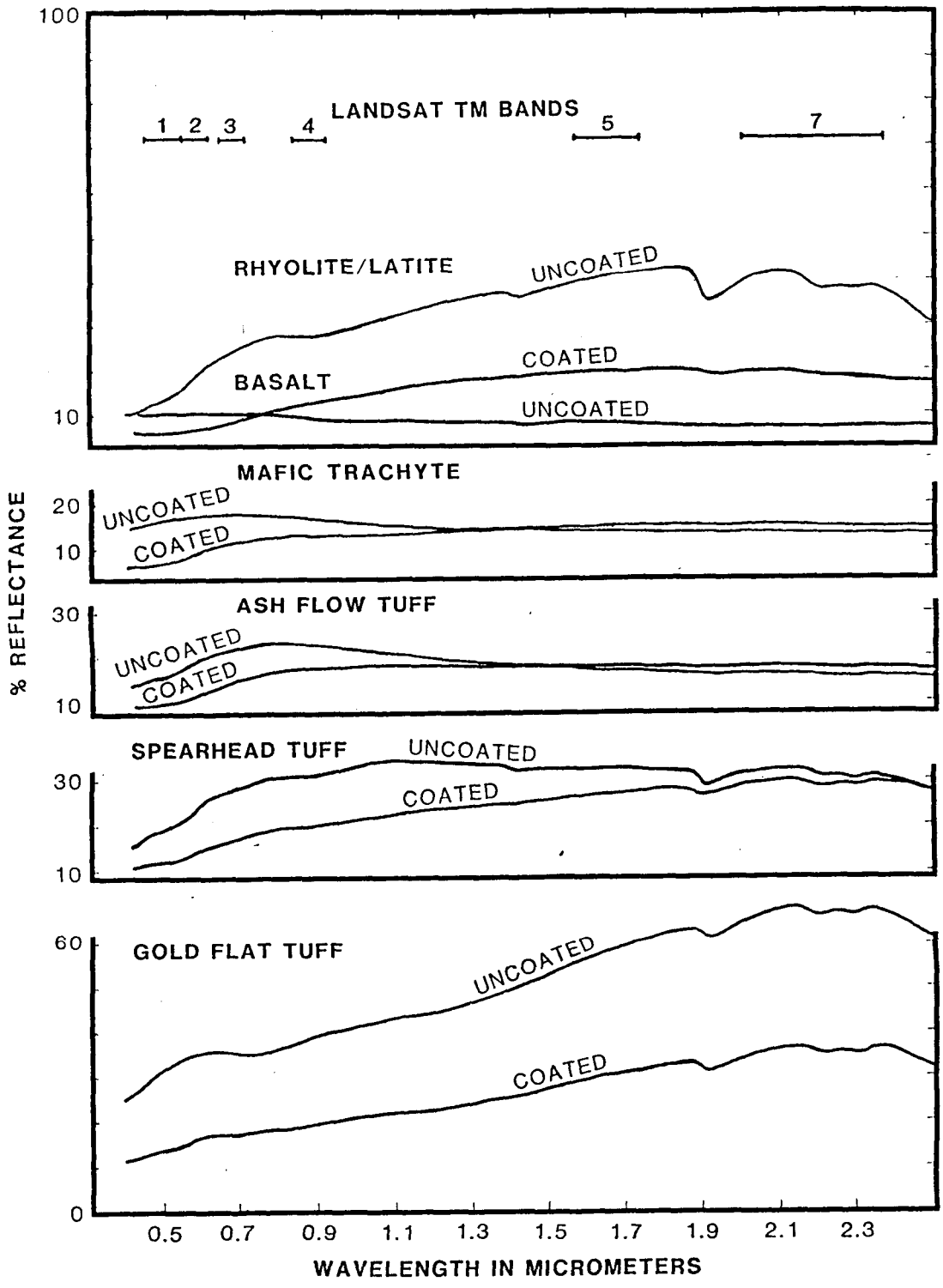

Figure 13. Spectral curves of rock surfaces with extensive desert varnish compared with their unvarnished counterparts. Data collected on JPL's Beckman lab spectrophotometer. (Uncoated sample only shown for the rhyolite sample.)

PRECEDING PAGE BLANK NOT FILMED

concentration of incompatible LIL elements, between bands 5 and 7 is quite steep, which should lead to very low 5/7 values.

6. Felsic units with a high concentration of varnish should exhibit higher 5/2 values.

These relationships help explain imagery contrast and band relationships at each of the 3 study sites where similar relationships exit with regard to desert varnish occurrence, magmatic evolution, and petrochemistry. The following 2 sections present binary and ternary plots which exhibit these relationships, graphically.

LITHOLOGY-PETROCHEMISTRY-BAND REFLECTANCE DIAGRAMS

Figures 14, 15, and 16 show reflectance values for each of the TM bands of each lithologic unit worked with to date. Figures 17, 18, 19 and 20 present binary and ternary band vs band plots and band vs composition diagrams for units from the Stonewall Mountain area. The focus was on bands which seemed most significant from imagery and lab spectra. Although points on the graphs are limited by the restricted number of mappable imagery units in the scenes, some unapparent trends and groupings of units can be delineated on the basis of expected relationships involving felsic tendencies, degree of magmatic evolution, and extent and maturity of desert varnish. The trends and groups that are interpreted on these diagrams and those that follow are consistent with the imagery and lab spectra for these units.

The more magmatically evolved late flows of the Stonewall Mountain caldera - the ash flow tuffs - show lower 5/7 values than the basalts and rhyolites dervived from the Mount Helen caldera (Figure 17). Although a straight line albedo relationship exists amoung the units on the 5 vs 7 plot, divergence on the other graphs seem to follow 2 distinct trends: one involving the ash flow of the Stonewall caldera, the other involving the units from Mount Helen. The lower 5/7 values of the ash flow units of Stonewall is probably due both to the existence of more extensive, well developed desert varnish on these units and to the relatively high concentration of incompatible elements they contain. The two groups plot along separate trends on the 2 vs 5 graph, due apparently to absorption of varnish in band 2. The higher albedo of more felsic and evolved units leads to the trends within each of the two groups. The 5/2 vs 7 diagram distributes the units in a broad relationship congruent with magmatic evolution - higher 7 and 5/2 values.

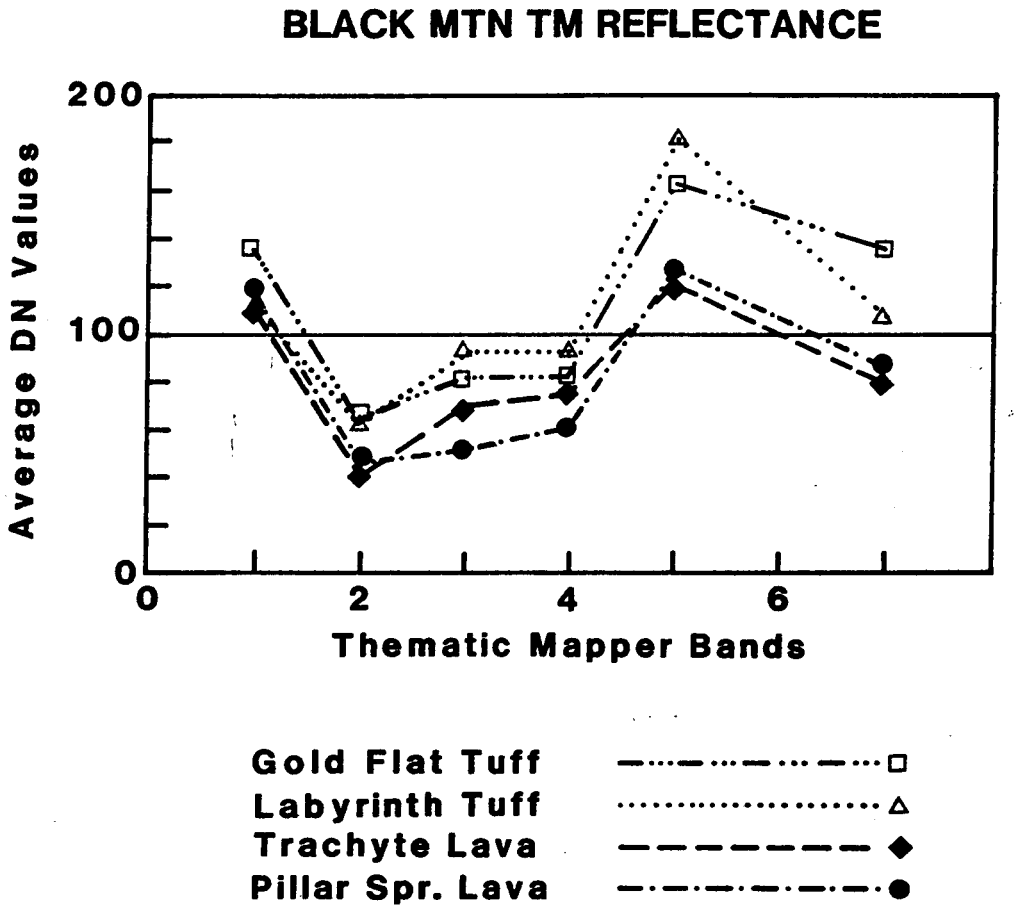

Figure 14. Reflectance values by TM band for each unit of the Black Mountain site DN values are for well illuminated exposure

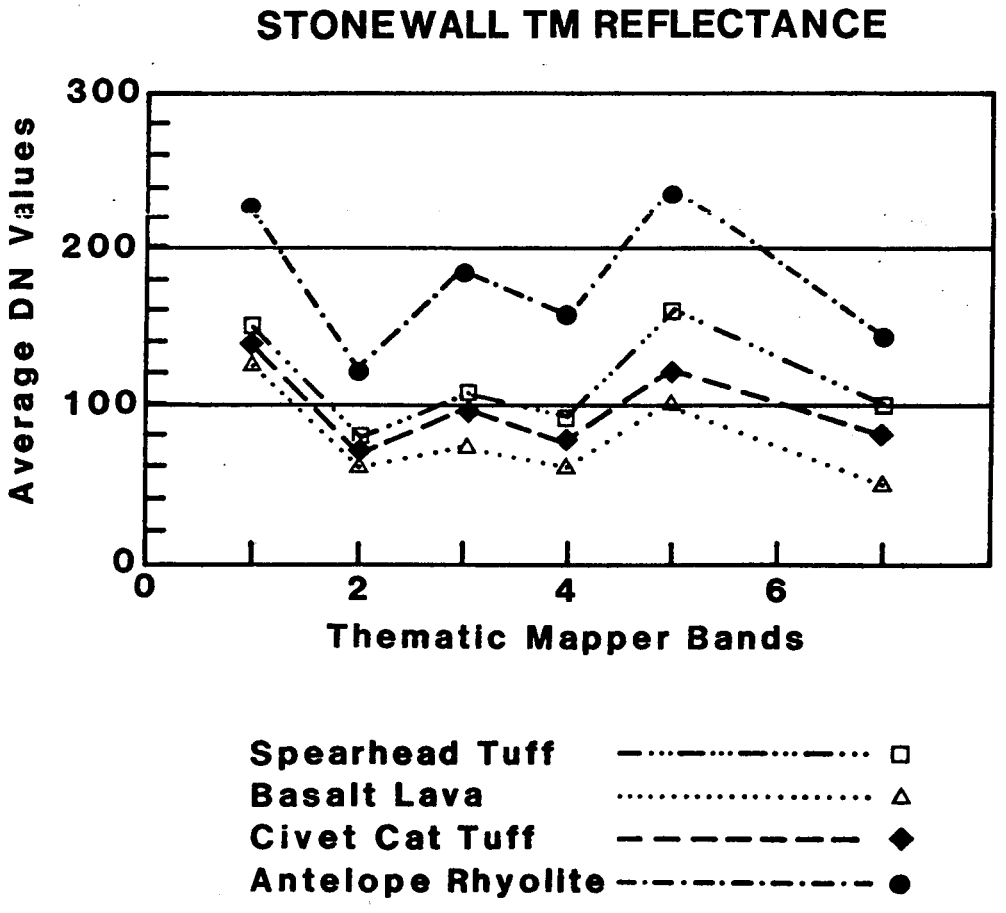

Figure 15. Reflectance values by TM band for units from Stonewall Mountain. DN values are for well illuminated exposure.

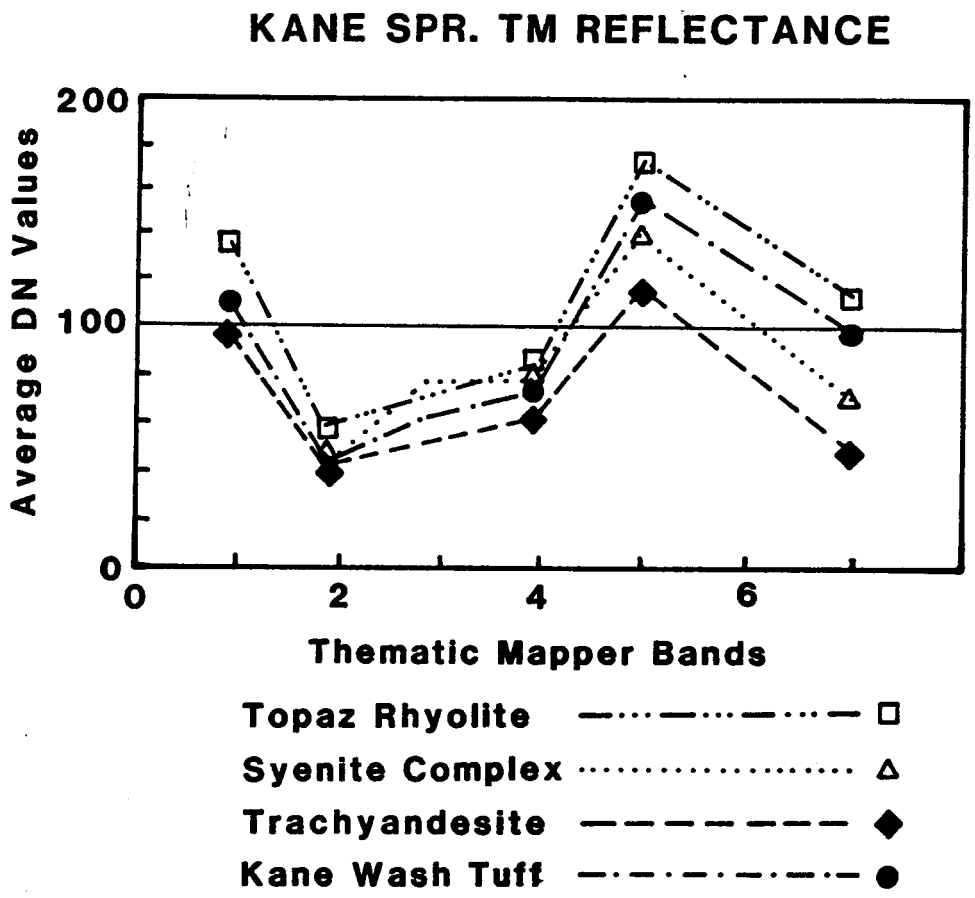

Figure 16. Reflectance values by TM band for units from the Kane Springs Wash site. DN values are for well illuminated exposure.

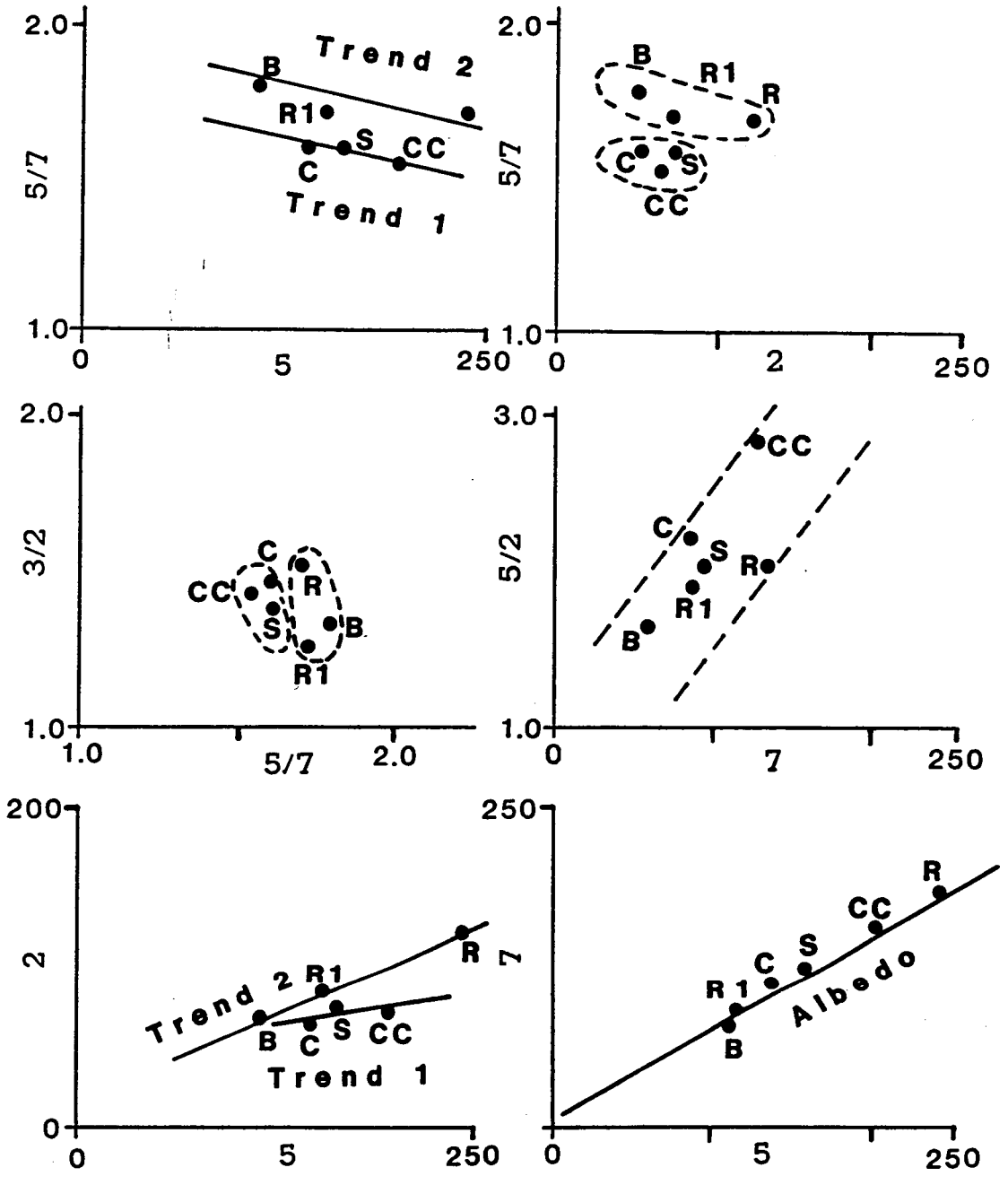

B - Late Basalt
S - Spearhead Tuff
C - Civet Cat Canyon Tuff
CC - Civet Cat Canyon Cap Rock
R - Antelope Springs Rhyolite
R1 - Antelope Springs Lower Rhyolite

Figure 17. Band vs band plots for lithologic units from the Stonewall Mountain site.

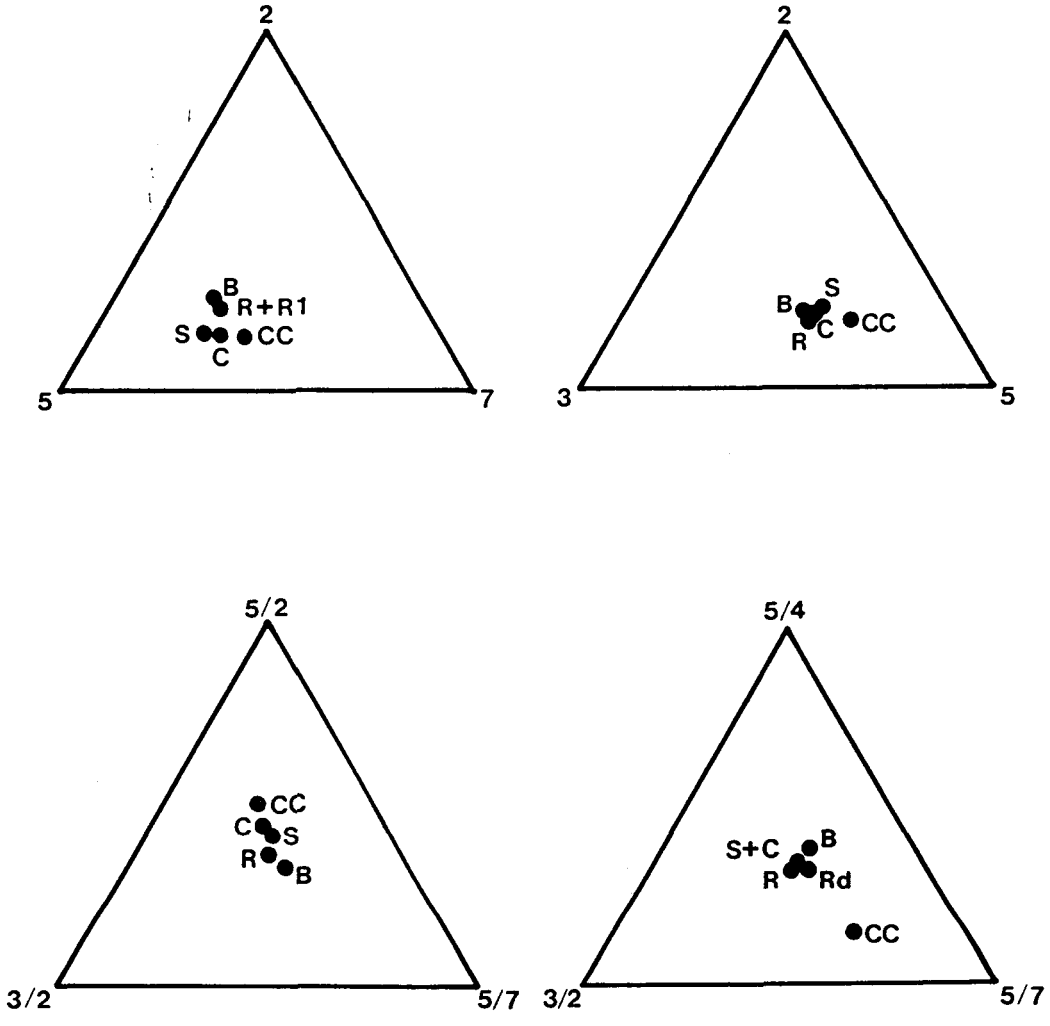

B - Late Basalt
S - Spearhead Tuff
C - Civet Cat Canyon Tuff
CC - Civet Cat Canyon Cap Rock
R - Antelope Springs Rhyolite
R1 - Antelope Springs Lower Rhyolite

Figure 18. Ternary plots of bands and band ratios from the Stonewall site showing the more prominent lithologies.

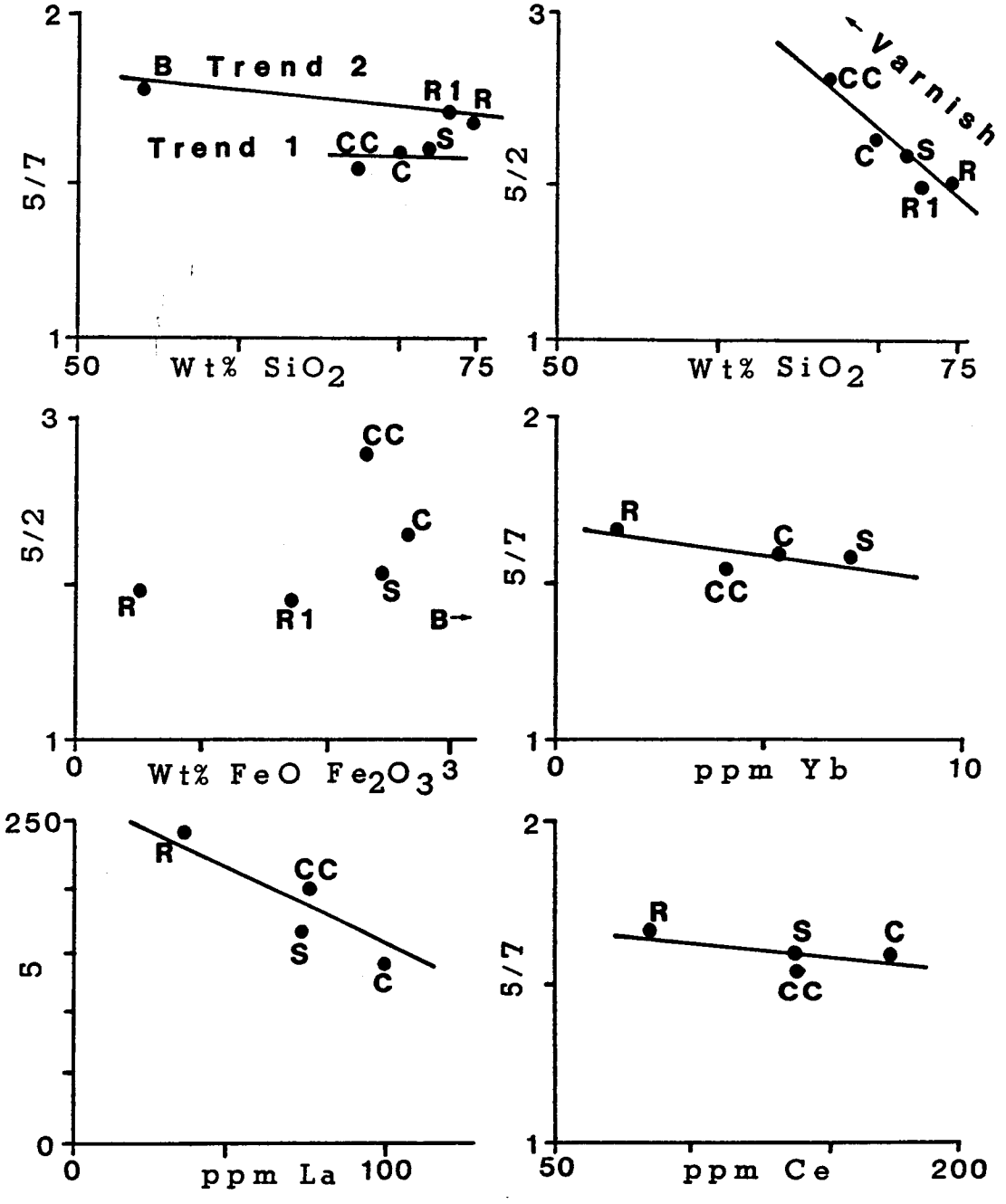

B - Late Basalt
S - Spearhead Tuff
C - Civet Cat Canyon Tuff
CC - Civet Cat Canyon Cap Rock
R - Antelope Springs Rhyolite
R1 - Antelope Springs Lower Rhyolite

Figure 19. Plots of band values vs compositional properties of various units from the Stonewall area.

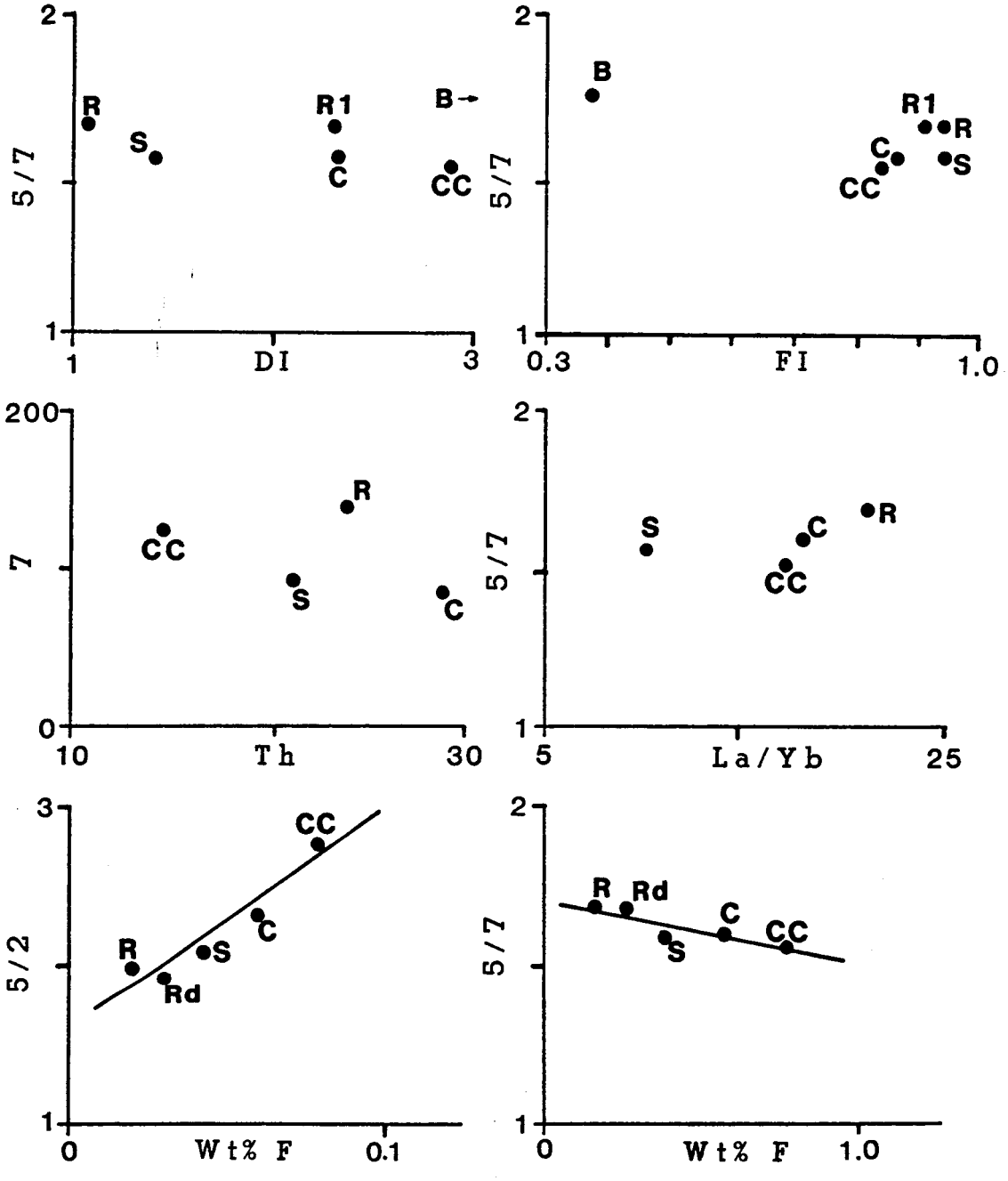

B - Late Basalt
S - Spearhead Tuff
C - Civet Cat Canyon Tuff
CC - Civet Cat Canyon Cap Rock
R - Antelope Springs Rhyolite
R1 - Antelope Springs Lower Rhyolite

Figure 20. Diagrams of bands and band ratio DN values for the units from Stonewall Mountain plotted against compositional properties.

Ternary band plots for the Stonewall units (Figure 18) distribute the deposits in predictible patterns according to relationships depicted in the binary diagrams. the linear distribution on the 5/2-5/7-3/2 triangle is believed to be due in part to both rock petrochemistry, with the highly evolved units plotting away from the 5/7 apex and toward the 5/2 apex, and to desert varnish, with the ash flow tuffs falling toward the 5/2 apex.

Figures 19 and 20 show band vs compositional diagrams for the Stonewall units . Distinct trends result from a correlation of albedo with felsic tendency, enrichment in incompatible elements and thus degree of magmatic evolution, and extent and intensity of desert varnish. It seems worthy to note that reflectance trends of 5/7 and 5/2 ratios with respect to silica indicate a slight negative slope and increase in silica with a decrease in 5/7 values as expected, but 5/2 ratios decrease as well, and sharply, as silica increases. As we will see from plots of values from the other 2 study sites, an increase in 5/2 ratios seems to indicate an increase in magmatic evolution, more as measured by peralkaline tendency (higher Na2O+K2O), rather than silica. Band reflectance plots against the rare elements reveals linear relationships particularly between 5/7 values and F. The correlation between reflectance values and the rare elements is superior to linear relationships between reflectance values and the major oxides, reflected in part by the differentiation index (DI) and Felsic index (FI).

Similar relationships and trends can be found among the band vs band and band vs compositional plots for units from the Black Mountain and Kane Springs Wash study sites (Figures 21-28). At Black Mountain, highly evolved peralkaline Gold Flat Tuff and Labyrinth Canyon Tuff (distal Spearhead) form separate trends and groups since they both have relatively high albedo and exhibit relatively well developed desert varnish. Both units have high values in band 5, low values in band 2, thus a high 5/2 ratio (Figure 21). The Gold Flat Tuff is an unusual, quite highly evolved late magmatic differentiate with a low 5/7 ratio and high F and alkaline components (Figure 23). The ternary plot of 5/4-5/7-3/2 distributes deposits according to alkaline tendencies and incompatible element content, with lowest to highest from Trachyte of Hidden Cliff (T), lavas of Pillar Springs and Trail Ridge Tuff (PR), older Thirsty Canyon Tuff (C), Labyrinth Canyon Tuff (L), to Gold Flat Tuff (G). The correlation between lower 5/7 values with degree of magmatic maturity is again apparent in reflectance vs rare element plots, particularly Th, Rb, and F (Figures 23 and 24).

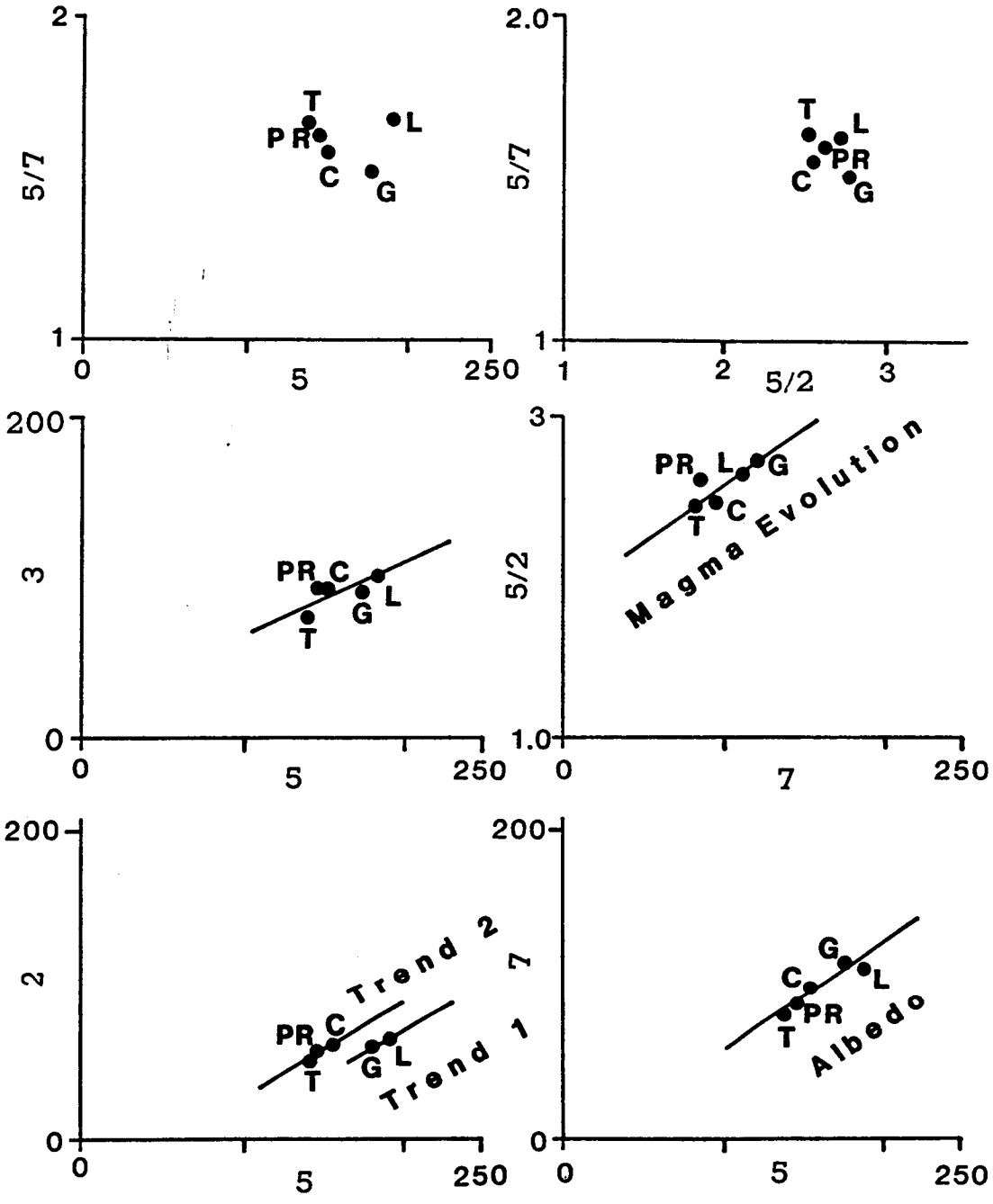

L- Labyrinth Canyon Tuff
G - Gold Flat Tuff
T - Trachyte of Hidden Canyon
PR - Lava of Pillar Springs and Trail Ridge Tuff
C - Older Thirsty Canyon Tuffs

Figure 21. TM band DN plots for the various units from the Black Mountain site.

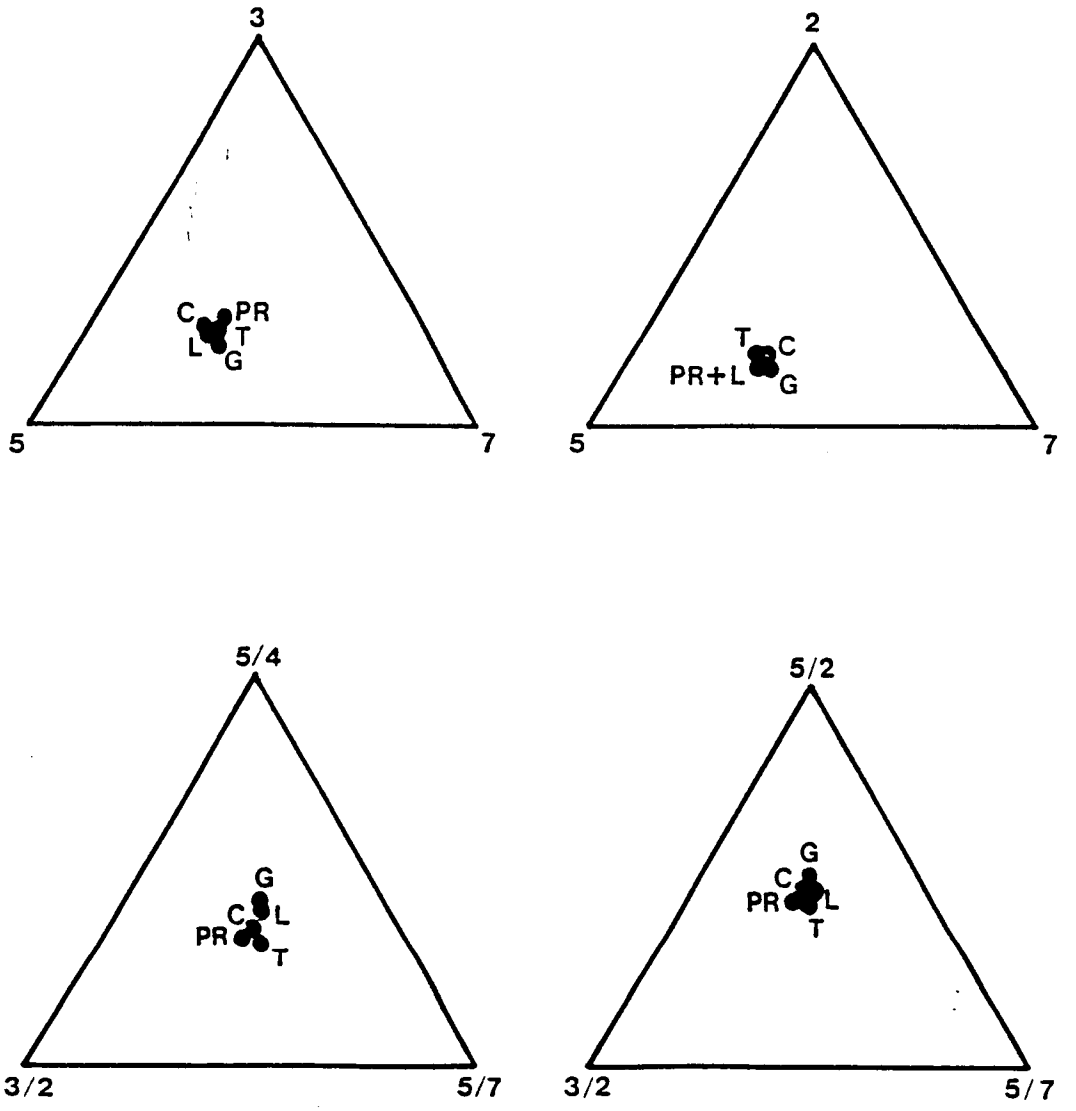

L- Labyrinth Canyon Tuff
G - Gold Flat Tuff
T - Trachyte of Hidden Canyon
PR - Lava of Pillar Springs and Trail Ridge Tuff
C - Older Thirsty Canyon Tuffs

Figure 22. Ternary diagrams of TM band DN values for units from the Black Mountain site.

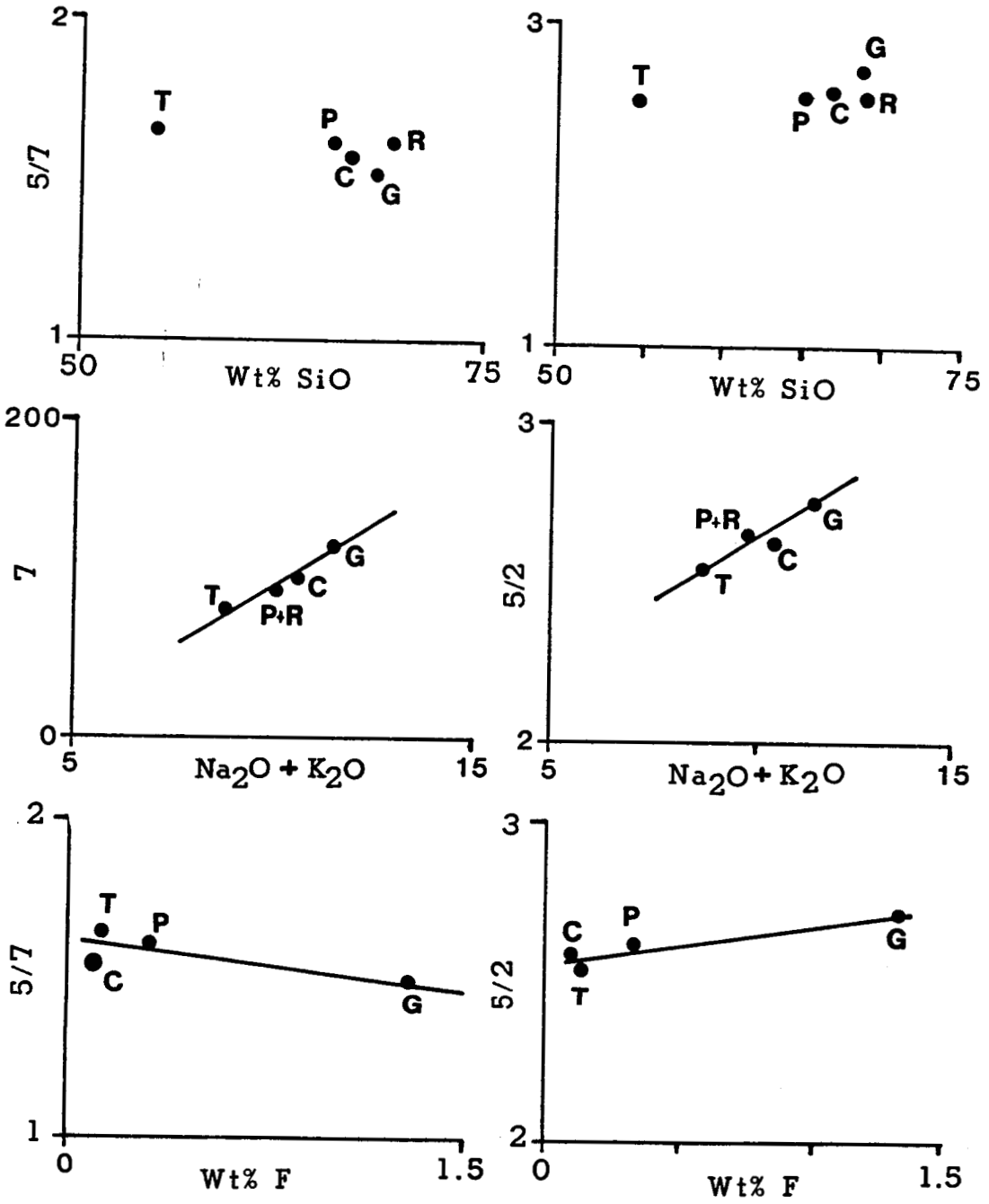

G - Gold Flat Tuff
R - Trail Ridge Tuff
P - Lava of Pillar Springs
T - Trachyte of Hidden Cliff
C - Older Thirsty Canyon Tuffs

Figure 23. Binary diagrams plotting TM DN values of various geologic units of the Black Mountain site against compositional properties.

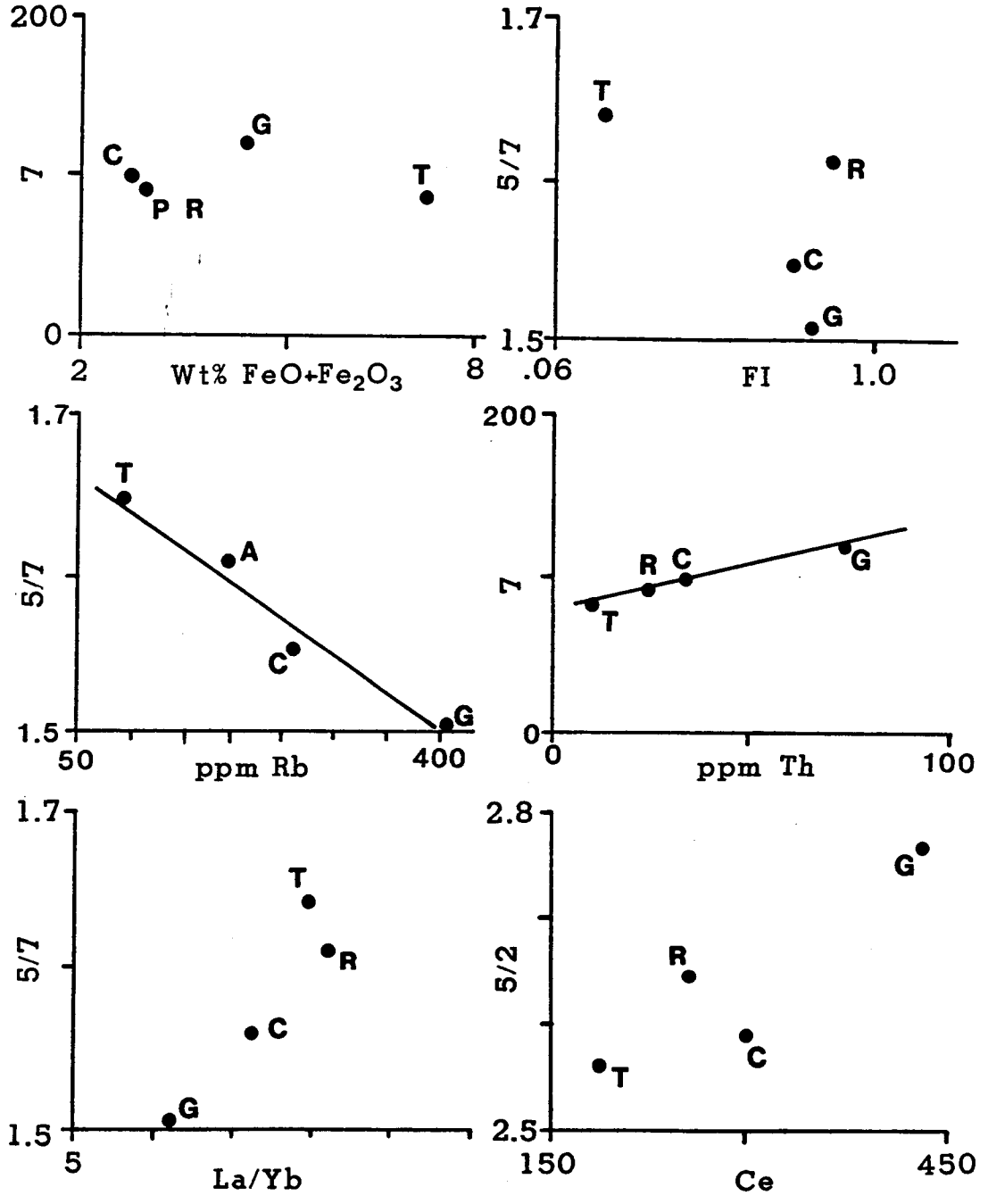

G - Gold Flat Tuff **T - Trachyte of Hidden Cliff**
R - Trail Ridge Tuff **C - Older Thirsty Canyon Tuffs**
P - Lava of Pillar Springs

Figure24. Binary plots showing TM DN values vs compositional characteristics of various units from the Black Mountain site.

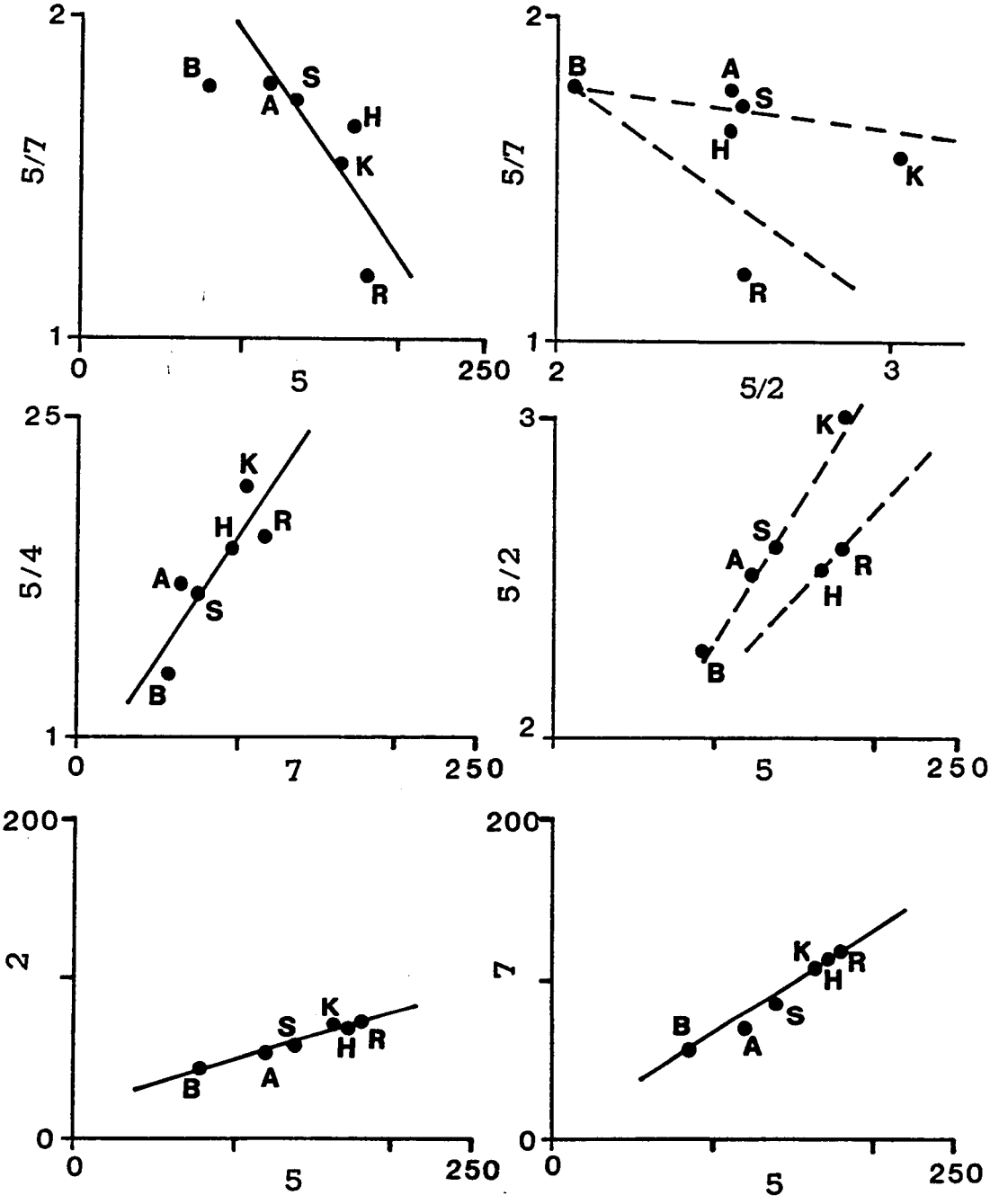

R - Topaz Rhyolite
B - Basalt Flow
A - Trachyandesite
H - Hico Tuff
K - Kane Wash Tuff (V)
S - Syenite Complex

Figure 25. Band vs band and band ratio DN relationships for the various units at Kane Springs Wash.

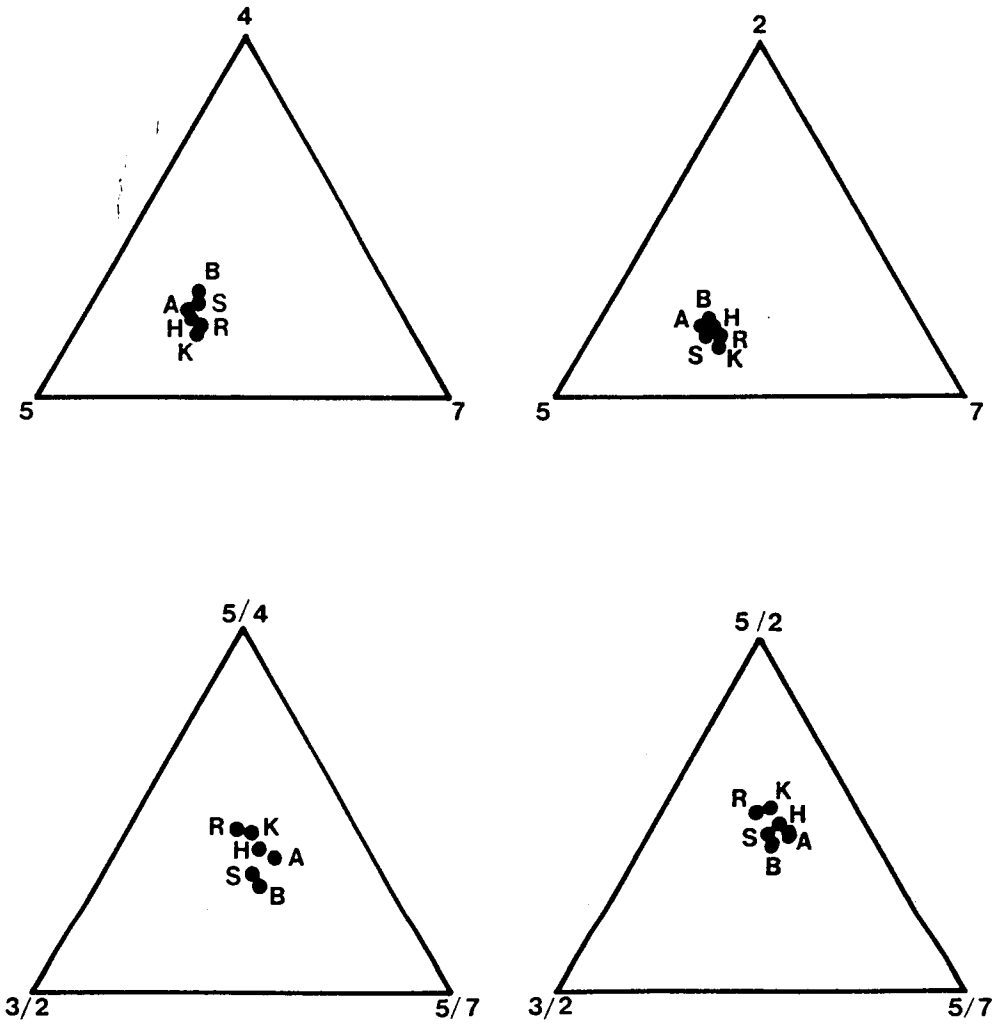

R - Topaz Rhyolite
B - Basalt Flow
A - Trachyandesite
H - Hico Tuff
K - Kane Wash Tuff (V)
S - Syenite Complex

Figure 26. Ternary relationships among DN values for TM bands and band ratios for various geologic units from the Kane Springs Wash site.

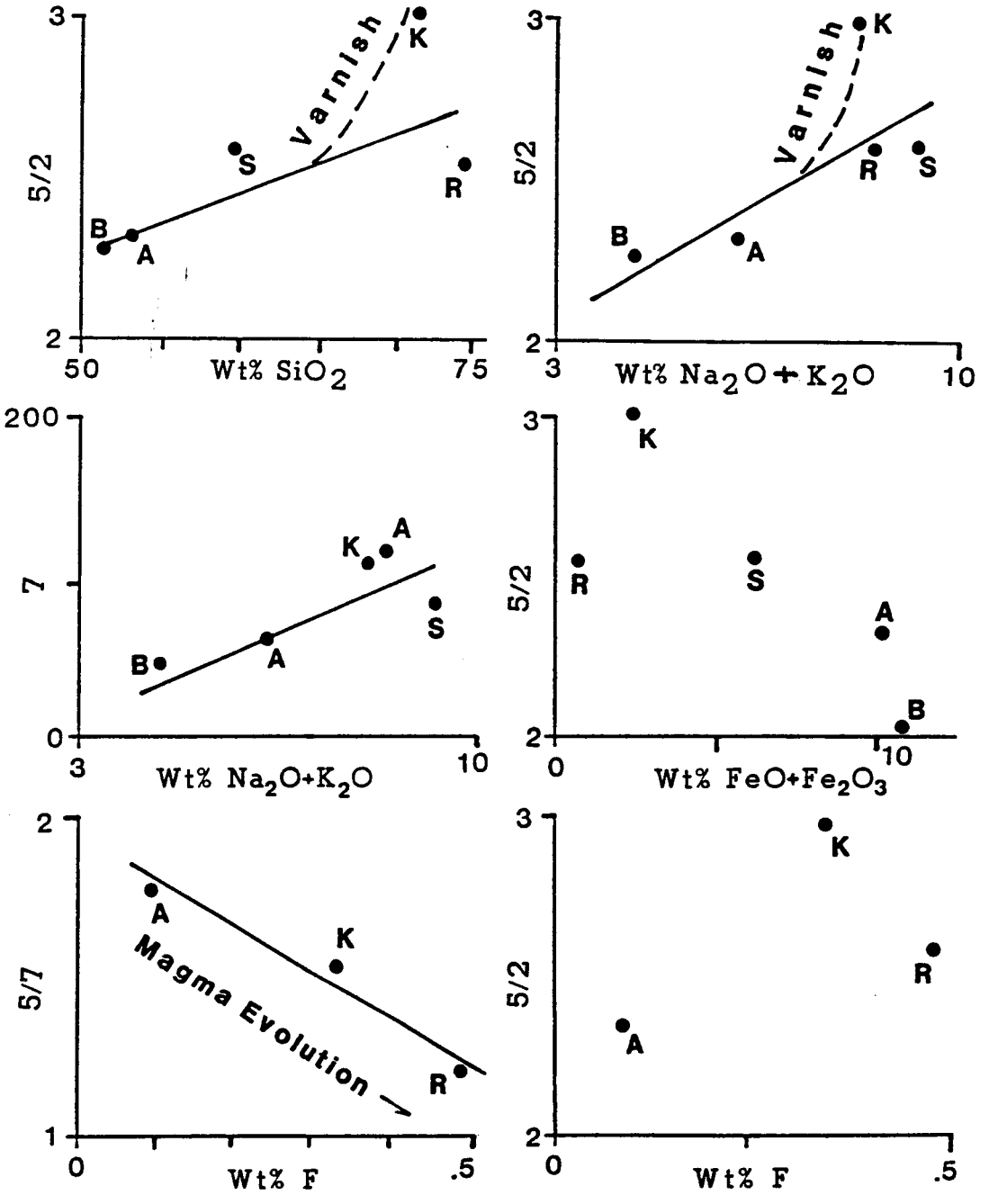

R - Topaz Rhyolite
B - Basalt Flow
A - Trachyandesite
H - Hico Tuff
K - Kane Wash Tuff (V)
S - Syenite Complex

Figure 27. Binary diagrams showing band and band ratio DN values of TM imagery over lithologic units of the Kane Springs site.

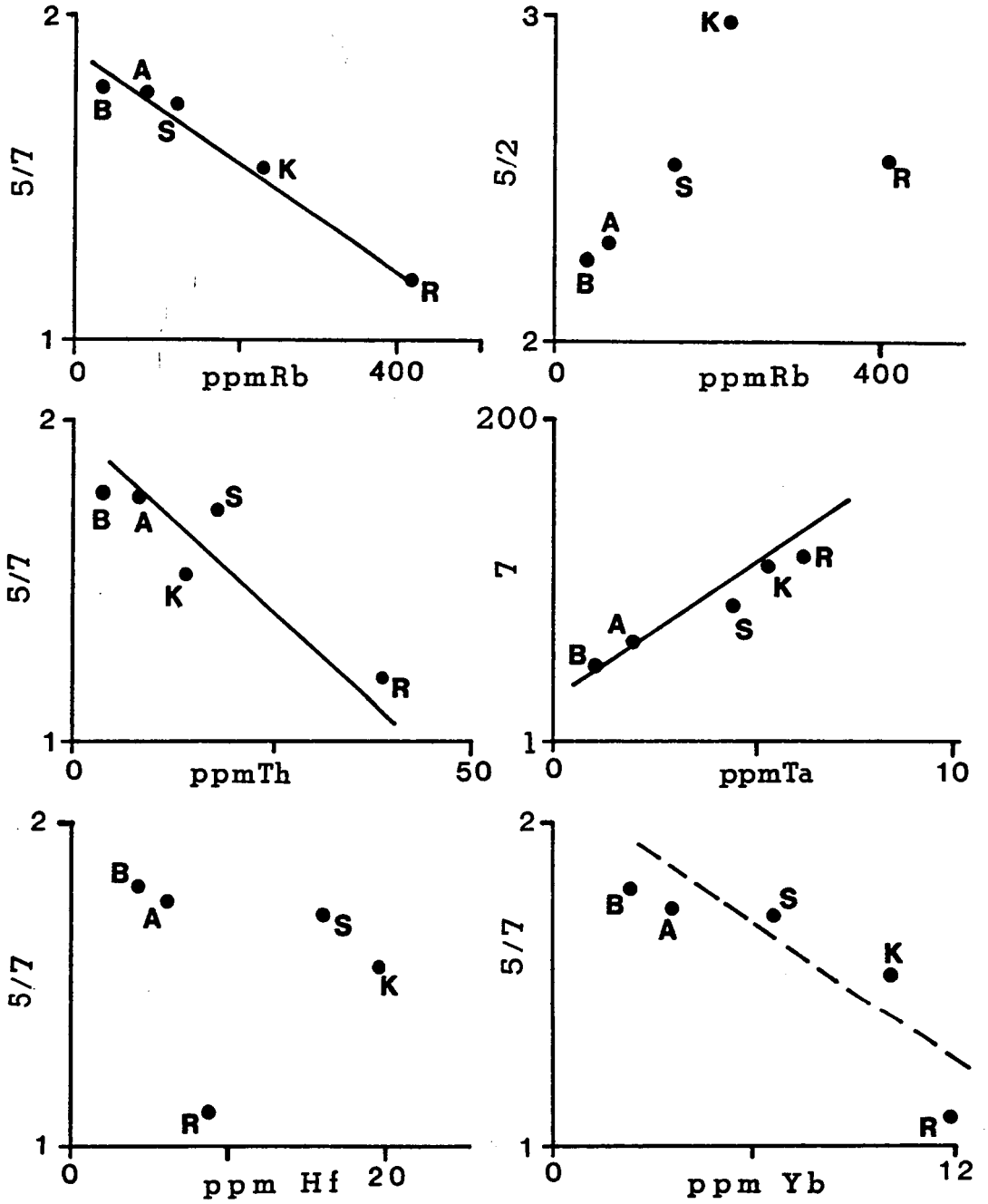

Figure 28. TM DN values over lithologic units from the Kane Springs Wash site plotted against compositional properties.

At Kane Springs Wash interesting spectral characteristics are apparent between the 3 highest albedo units, the Hico Tuff, Kane Springs Tuff, and Topaz Rhyolite which are congruent with differences in tendencies toward magmatic maturity and desert varnish formation. The final flow from the Kane Springs volcanic center was the Kane Springs Tuff which consisits of 3 cooling units. Each is peralkaline and faily well evolved. They were follosed by intracaldera lava domes consisting of topaz rhyolite, the most evolved deposit of the center. Divergencies exit from the more typical plots established among the units at the other 2 study sites. On a 5/7 vs 5 plot, for example (Figure 25), a good linear correlation exits, compatible with magmatic evolution, whereas on the 5/7 vs 5/2 plots, Kane Wash Tuff and topaz rhyolite appear to plot along divergent trends due possibly to the greater development of desert varnish and higher 5/2 values on the former. More extensive varnish may account for the departure of Kane Wash Tuff from an otherwise linear distribution on the 5/2 vs Na2O+K2O and 5/2 vs SiO2 diagrams (Figure 27). Again the large ion lithophile (LIL) elements and other incompatibles provide positive correlation with band 7 and 5/7 plots. Particularly good linear relationships are exhibited with Ta, Rb, Yb, and F.

Figures 29 and 30 combine units from each of the study areas. In these diagrams the relationships established for each area seem to prevail in a general way. A felsic and magmatic evolution trend seem to give birth to both lower 5/7 and higher 5/2 values; the 5/7 relationship dominating in importance. Trend bifercations interpreted from the binary graphs (Figure 30) reflect higher 5/2 ratios over units with well developed varnish and lower 5/7 values with an increase in peralkalinity and rare element content. Higher albedos in bands 5 and 7 follow a general increase in felsic tendencies.

THE ROCK-VARNISH INDEX

With an increase in desert varnish formation on a given host, both in terms of intensity or thickness and pervasiveness, there should also be a concomittant increase in the 5/2 ratio IF a significant difference exists between the composition and albedo of the varnish and that of the underlying host. As host felsic tendency increases so too would reflectance values increase as wavelength increases. With an increase in thickness of varnish, reflectance would be increasingly attenuated due to increased absorption by varnish relative to underlying host. Varnish coatings on mafic rocks appears indistinguishable due to similarities in albedo. The varnish divergence trends interpreted on the

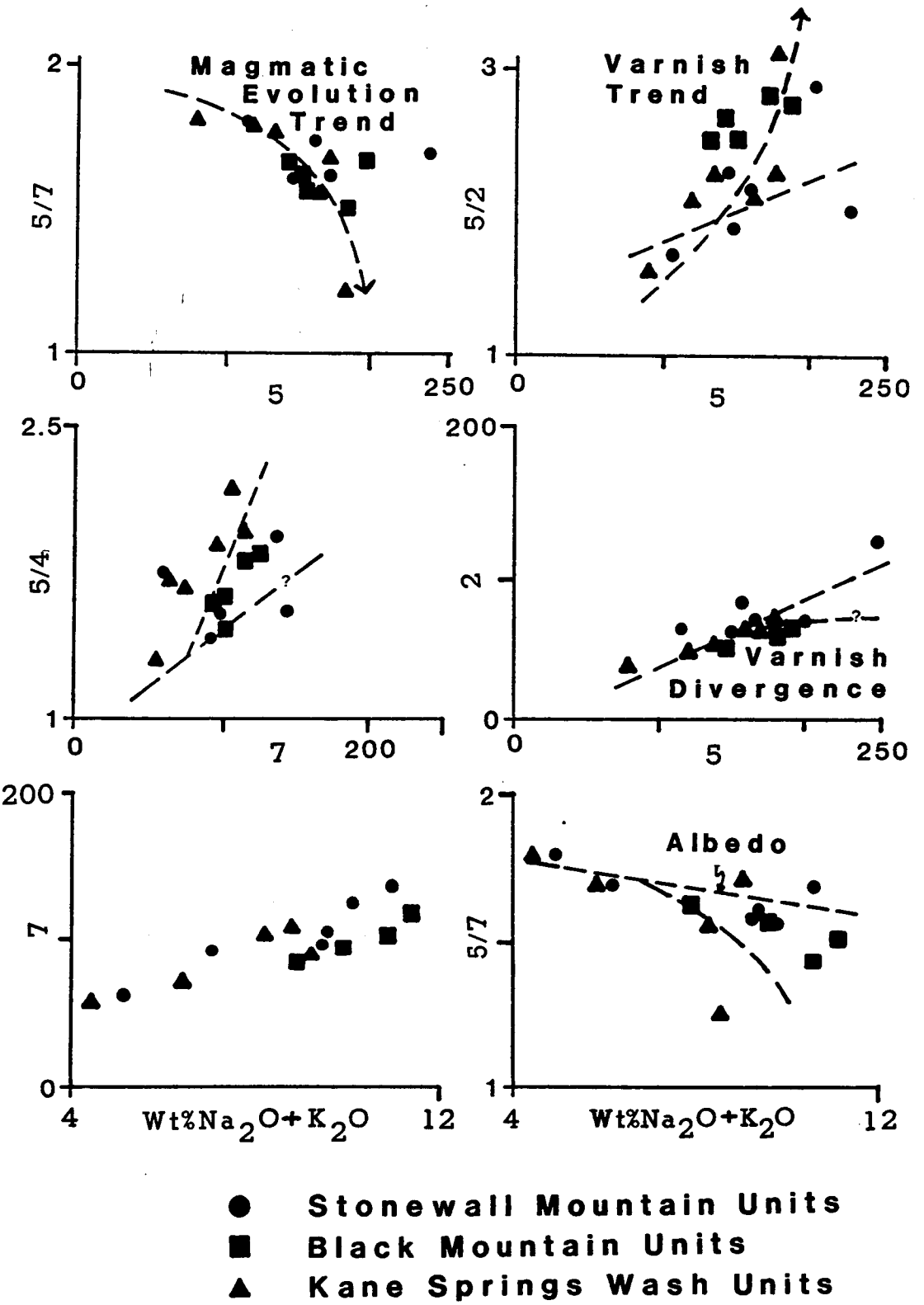

Figure 29. Units of the 3 study sites combined on binary plots in order to show some apparent unifying relationships.

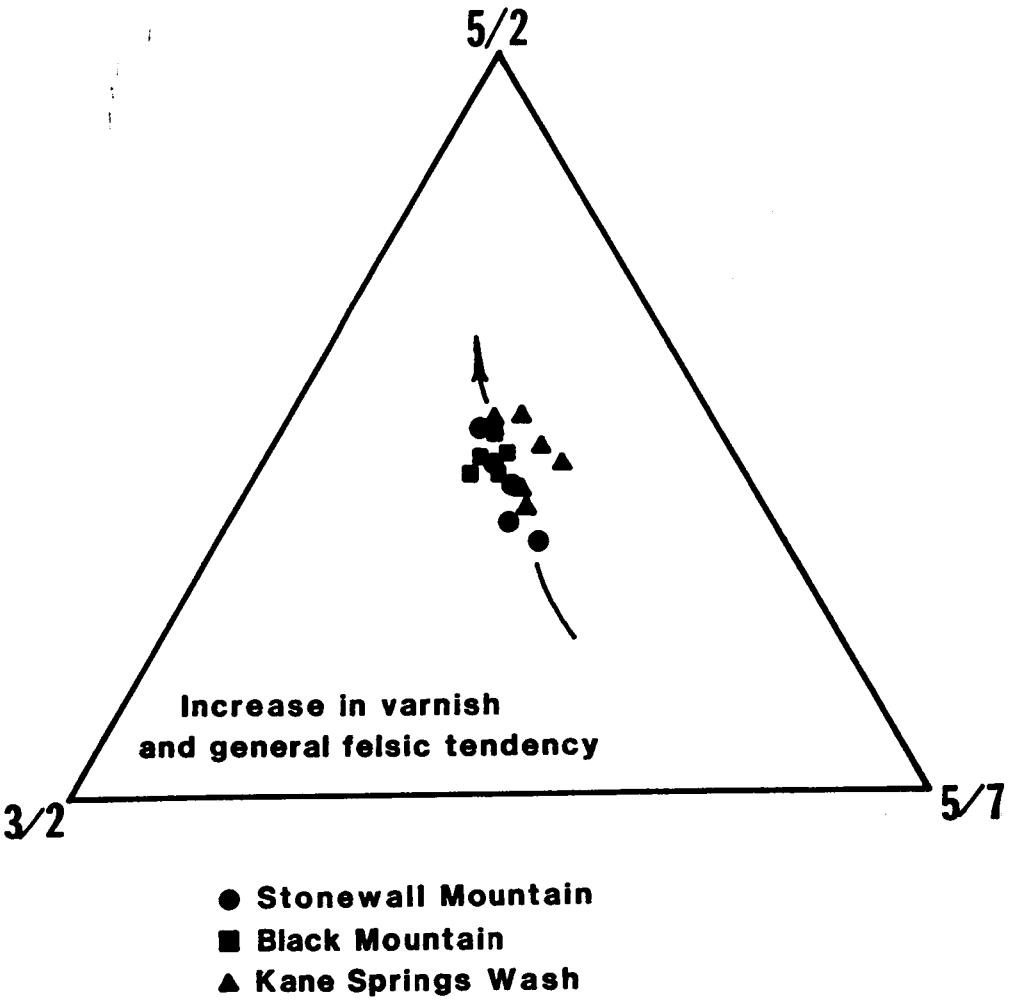

Figure 30. Ternary plot of band ratios showing possible trend related to increase in desert varnish and felsic tendency.

graphs above are controlled by both the difference in compositon between the varnish and host rock and the extent of varnish development. The 5/2 ratio can be a helpful measure of extent of varnish development. Its applicability increases with felsic tendency of host rock. Attenuation of reflectance by varnish is inversely proportional to wavelength. As varnish builds up on a given host, bands 2 and 5 are disproportionately affected, with shorter wavelengths affected the greater. This should result in a hyperbolic curve relationship if varnish thickness were plotted against a 5/2 ratio to a point where band 2 reflectance reaches a minimum and the curve slope stabilizes.

It seems useful to introduce a new concept that should help our discussions of varnish and its imagery characteristics. The detection of varnish, according to principles discussed above, depends on the compositional difference between the varnish and underlying host. This difference, perhaps best defined in terms of the ferromagnesian components is herein termed the Rock-Varnish Index (RVI) defined by:

$$RVI = \frac{wt\%\ MnO + FeO \text{ in varnish}}{wt\%\ MnO + FeO + Fe2O3 + MgO \text{ in host}}$$

A plot of the 5/2 ratio and RVI's for several units is shown in Figure 31. Varnish compositions were probed by a scanning electron microscope with an energy dispersive X-ray system. Since SEM analysis is typically inaccessible to many investigators it is useful to realize that the FeO+MnO content of varnishes we have investigated remains fairly constant - 40-50% - on felsic units. The RVI, therefore, for our suite of volcanic rocks is determined chiefly by the felsic tendency of host rather than by variations of Fe and Mn in the varnish. For sake of desert varnish identification by TM imagery, which largely involves detecting a difference between varnish and host composition, we can say that the more felsic rocks have a high RVI potential.

CONCLUSIONS

TM spectral characteristics of volcanic rock assemblages at the Stonewall Mountain, Black Mountain, and Kane Springs Wash volcanic centers are distinct and seem to correlate in part with both rock petrochemistry and extent of desert varnish. Supervised classification, involving IDIMS function CLASFY, was effective at the one site where it was applied, Stonewall Mountain, at discriminating mappable formations. Discrete classes trained on previously unmapped

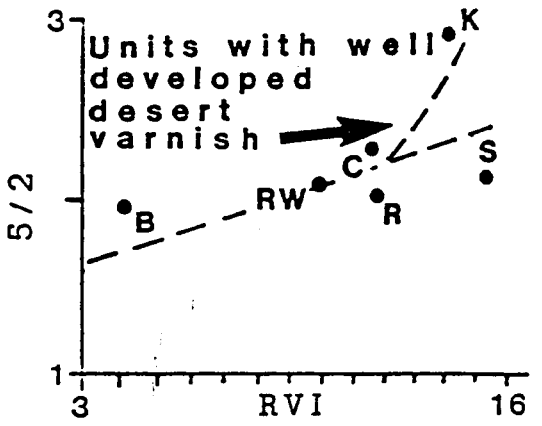

ROCK VARNISH INDEX

$$RVI = \frac{\text{Wt\% MnO+FeO in varnish}}{\text{Wt\% MnO+Fe}_2\text{O}_3^{+}\ \text{FeO+MgO in rock}}$$

Figure31. Plot of TM DN values for bands 5/2 against the RVI of several units. Varnish compostions were collected by SEM-EDX probs.

formations were consistently correlative with field observation and field mapping efforts. Directional filters aided identificaiton of thin airfall ash deposits at the base of both the Spearhead and Civet Cat Canyon Tuff deposits. Some reduction of vegetation reflectance in color composite images was accomplished by adding band ratios 4/3 and 5/4, in which vegetation is bright and dark, respectively.

Congruency between imagery contrast, Band DN values over the various lithologic units, lab spectra, and binary and ternary plots of band vs band and band vs compositions for the volcanic formations leads to discriminatory potential based largely on albedo in the longer wavelength bands and on 5/7 and 5/2 ratios. Figure 32 is a binary decision rule flow diagram for analysis of volcanic caldera settings in arid to semi-arid environments based on the results presented above.

Rocks with a high Rock-Varnsih Index RVI are felsic relative to desert varnish and thus bear potential for varnish identification. The RVI concept and high 5/2 values seem potentially applicable also to discrimination of felsic rocks with low albedos caused by factors such as matrix iron resulting from autooxidation or other secondary effects, from more mafic units with low straight line albedos and low 5/2 values.

ORIGINAL PAGE IS
OF POOR QUALITY

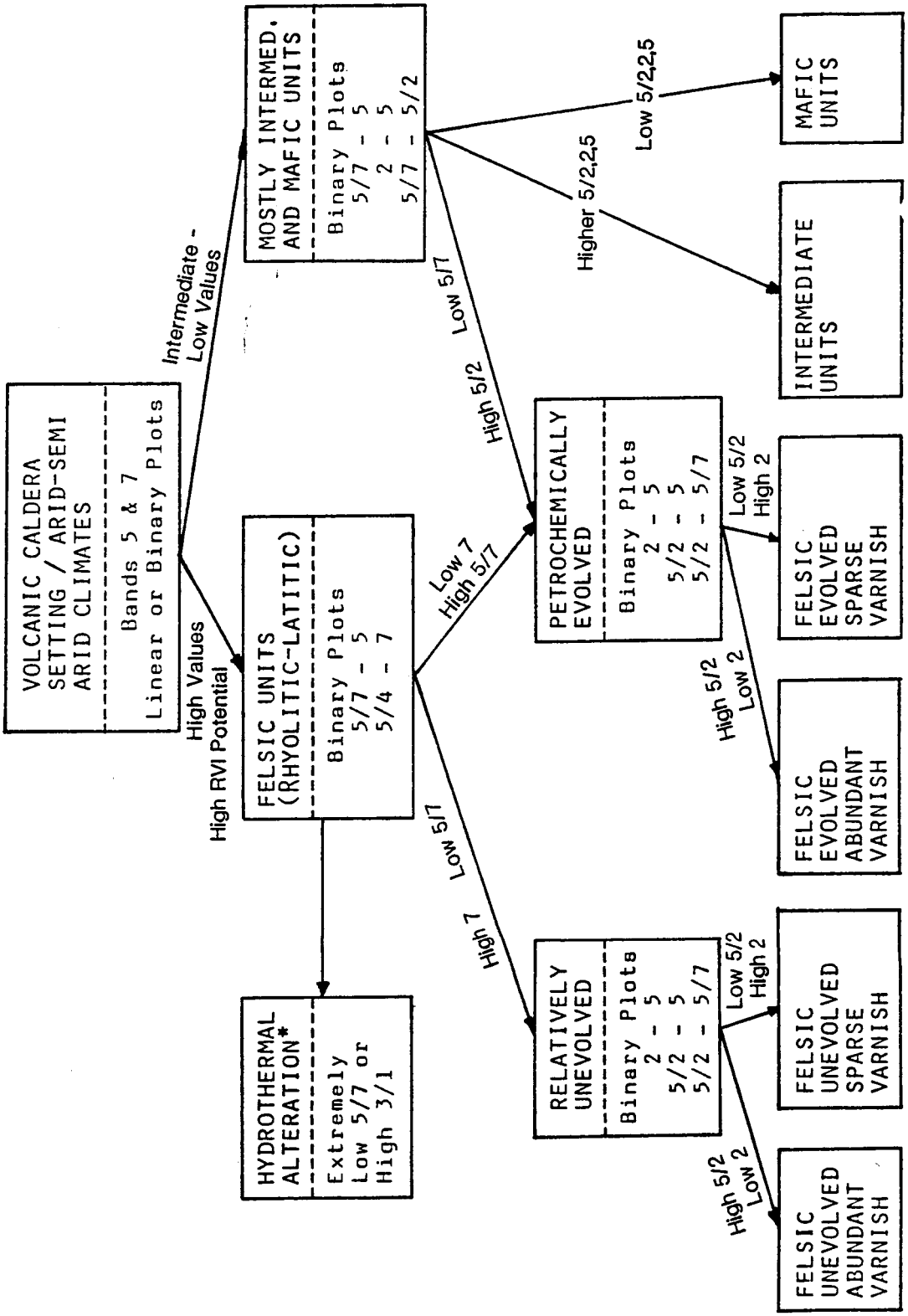

* TYPICALLY PERVASIVE ARGILLIC, SEICITIC, SILICIC, OR ALUNITIC ALTERATION WITH PYRITE

** EVOLVED RELATIVE TO PERALKALINE TENDENCY AND TRACE ELEMENT CONTENT, PARTICULARLY F, Rb, Ta, Th and REE

Figure 32. Binary decision-rule flow diagram to help lithologic discrimination within Tertiary caldera settings using Landsat TM imagery.

WORK PLANNED FOR NEXT REPORTING PERIOD

Efforts will continue over the next 6 months to further our understanding of petrologic, petrochemical, and desert varnish influence on TM spectra. An additional 26 samples have been selected for complete geochemical profiling, 12 additional desert varnish samples identified for microprobe analysis, and some 81 field spectra have been calibrated and plotted for evaluation, including comparisons between samples of the same unit with variable varnish distribution. Further supervised classification processing is being conducted on imagery over Black Mountain and Kane Springs, and a more focused imagery processing effort is being conducted on ratios of bands 2, 5 and 7 which tend to highlight both desert varnish and lithologies with distinctive petrochemistry. Geologic maps, based on remote sensing units, of each of the 3 areas are being compiled. Moreover, a more regional review of ash flow distribution around Stonewall Mountain is under investigation based on our imagery results. We are also collecting density measurements of different zones within weathering cortexes to refine mass balance calculations to enhance concepts on the origin of desert varnish.

REFERENCES

Buckingham, W.F. and Sommer, S.E., 1983, Mineralogical characterization of rock surfaces formed by hydrothermal alteration and weathering - application to remote sensing: Econ.Geol., v.78, pp.664-674.

Cook, E.F., 1965, Stratigraphy of Tertiary volcanic rocks in eastern Nevada: Nev. Bur. Mines Rept. No. 11, 61 p.

Cornwall, H.R., 1972, Geology and mineral deposits of southern Nye County, Nev.: Nev.Bur.Mines and Geol. Bull. 77. 49 p.

Davis, J.C.,1973, Statistics and data analysis in geology: John Wiley & Sons, N.Y.,N.Y., 2nd edit.,550p.

Dorn, R.I. and Oberlander, T.M., 1981, Microbial origin of desert varnish: Science, v. 213, p. 1245-1247.

Engel, C.G. and Sharp, R.P., 1958, Chemical data on desert varnish: GSA Bull., v.69, p.487-518.

Fontanel, A., Blanchet, C., and Lallemand, C., 1975, Enhancement of Landsat imagery by combination of multispectral classification and principal component analysis: Proceedings NASA Earth Res. Sur. Symp., July, 1975, Houston, Tex., TMX-58168, p.991-1012.

Haydn, R., Dalke, G.W., Henkel, J., and Bare, J.E., 1982, Application of the IHS color transform to the processing of multisensor data and image enhancement: presented at the Inter. Symp. on Remote Sensing of Arid and Semi-arid Lands, Cairo, Egypt, Jan. p.599-616.

Jensen, J.R., 1986, Introductory digital imagery processing: Prentice-Hall, Englewood Cliffs, N.J., 379 p.

Joreskog, K.G., Klovan, J.E., and Reyment, R.A., 1976, Geological factor analysis: Elsevier Scient. Pub. Co., N.Y.,N.Y., 178p.

Laudermilk, J.D., 1931, On the origin of desert varnish: Amer. Jour. of Science, v.21, p.51-66.

Noble, D.C., 1965, Gold Flat member of the Thirsty Canyon Tuff - a pantellerite ash-flow sheet in southern Nevada: U.S.G.S. Prof. P. 525-B, p.885-890.

Noble, D.C., Anderson, R.E., Ekren, E.B., and O'Connor, J.T., 1964, Thirsty Canyon Tuff of Nye and Esmeralda Counties, Nevada: U.S.G.S. Prof.P. 475-D, p.24-27.

Noble, D.C., 1968, Kane Springs Wash volcanic center, Lincoln County, Nev: GSA Mem. 110, p.109-116.

Noble, D.C., Vogel, T.A., Weiss, S.I., Erwin, J.W., McKee, E.H., and Younker, I.W.,1984, Stratigraphic relationships and source areas of ash-flow sheets of the Black Mountain and Stonewall Mountain volcanic centers, Nev.: Jour.Geoph.Res., v.89, p.8593-8602.

Novak, S.W., 1984, Eruptive history of the Kane Springs Wash volcanic center, Nevada: Jour.Geoph.Res., v.89, p.8603-8615.

Novak, S.W., 1985, Geology and geochemical evolution the Kane Springs Wash volcanic center, Lincoln County, Nevada: Unpub. Ph.D. thesis, Stanford Univ., Stanford, Calif., 173 p.

Podwysocki, M.H., Gunther, F.J., and Blodget, H.W., 1977, Discrimination of rock and soil types by digital analysis of Landsat data: NASA Goddard Space Flight Center, X-923-77-17, 37 p.